Chapter 5
Lateral Motion and Deformation Along the Dead Sea Transform

Zvi Garfunkel

Abstract This paper presents an updated summary of the history and shallow structure of the Dead Sea transform (DST) and its plate tectonic context. The DST formed in the Early Miocene as a transform boundary between the Sinai and Arabian plates. The lateral offset was ca. 105 km near the Dead Sea. Since the DST trace is irregular in map view, the lateral motion led to formation of a 10–80 km wide deformation zone along the plate junction. Thus, the structures along the DST can be interpreted within the framework of the Sinai-Arabia plate kinematics. South of ca. lat. 33° transtension, which increased with time, led to variable oblique separation of the plate edges. This produced an almost continuous ca. 5–25 km wide depression whose structure is dominated by a string of pull-apart basins up to 15–20 km wide and up to ca. 12 km deep. The crystalline crust under the largest basins was appreciably thinned and may have been intruded by basalts. The structural pattern changed over time, the present pattern having been mostly established in the second half of the DST history. North of lat. ca. 33°N transpression dominates and the DST flanks are strongly deformed by folding, faulting, and rotation of fault blocks on vertical axes, which together produce shortening perpendicular to the DST and also left lateral shearing of its flanks, qualitatively compatible with the plate kinematic. The deformation can also account for the observed decrease of the lateral offset along the main fault line from ca. 100 km at ca. lat 33°N to 65–70 km at lat. 36°–36.5°N, and also leads to left lateral shearing along the continental margin near the Galilee and farther north. North of lat. 36.5°N the DST now interacts with the Anatolian plate and the Cyprus arc. This resulted from a rearrangement of the plate configuration in that region when westward extrusion of Anatolia began and the East Anatolian Fault formed, but the details of the kinematic changes are incompletely known. This change obscured the structural relations in this region during the early stages of the DST history.

Z. Garfunkel (✉)
The Fredy and Nadine Herrmann Institute of Earth Sciences, The Hebrew University of Jerusalem, Edmond J. Safra campus, 91904 Givat Ram, Jerusalem, Israel
e-mail: zvi.garfunkel@mail.huji.ac.il

Z. Garfunkel et al. (eds.), *Dead Sea Transform Fault System: Reviews*,
Modern Approaches in Solid Earth Sciences 6, DOI 10.1007/978-94-017-8872-4_5,

Keywords Dead Sea Transform • Strike slip faults • Plate motions • Pull aparts • Transpression

5.1 Introduction

The Dead Sea transform (DST) (also called Dead Sea or Levant Fault Zone), is one of the new plate boundaries produced by the mid-Cenozoic breakup of the once continuous African-Arabian continent. It forms the NW boundary of the Arabian plate, extending from the Red Sea spreading center to the zone of plate convergence in southern Turkey, a distance of ca. 1,000 km (Fig. 5.1). It is dominated by left lateral motion, ca. 105 km along its southern half. On the west most of the DST is delimited by the Sinai (sub-) plate, but its northernmost part also interacted with the Cyprus arc. The lateral motion along the DST was combined with minor, laterally variable, transtension or transpression which produced a deformed belt along its trace.

The DST attracted geologists already more than 150 years ago, and was recognized as the northern branch of the rift system that extends along East Africa and farther north (Suess 1891; Gregory 1921). At first the DST was interpreted as an extensional rift because parts of it are marked by valleys bordered by normal faults (Gregory 1921; Picard 1943). However, over time it was recognized that left-lateral slip dominates along the DST, so it is a transform plate boundary (Dubertret 1932; Quennell 1959; Freund 1965; Wilson 1965), but the traditional terms "Dead Sea rift" or "Dead Sea fault" are still sometimes used.

The purpose of this work is to present an updated summary of the shallow structure along the DST and how it is related to the lateral motion and to highlight important unsolved issues. Some other important topics are treated in companion papers in this volume.

5.2 Regional Setting

The DST crosses a continental area that was shaped by the Neoproterozoic Pan-African orogeny (Bentor 1985; Garfunkel 1988, 1999; Stern 1994). Later the region became a part of the stable North African-Arabian platform on which an extensive sediment cover accumulated in several depositional phases between Early Cambrian to mid-Cenozoic times (Picard 1943; Bender 1974; Brew et al. 2001a; Garfunkel 1988; Guiraud et al. 2001). Rifting events in latest Paleozoic and early Mesozoic times (ca. 270 to ca. 170 Ma) produced the passive margins of Arabia and NE Africa, including the Levant basin margin and the adjacent east Mediterranean basin (Bein and Gvirtzman 1977; Garfunkel and Derin 1984; Garfunkel 1998; Garfunkel and Ban Avraham 2001; Gardosh et al. 2010). Early Cretaceous intraplate igneous activity and uplifting occurred in the area crossed by the future DST (Garfunkel 1989; Segev 2009), but later there was hardly any igneous activity until

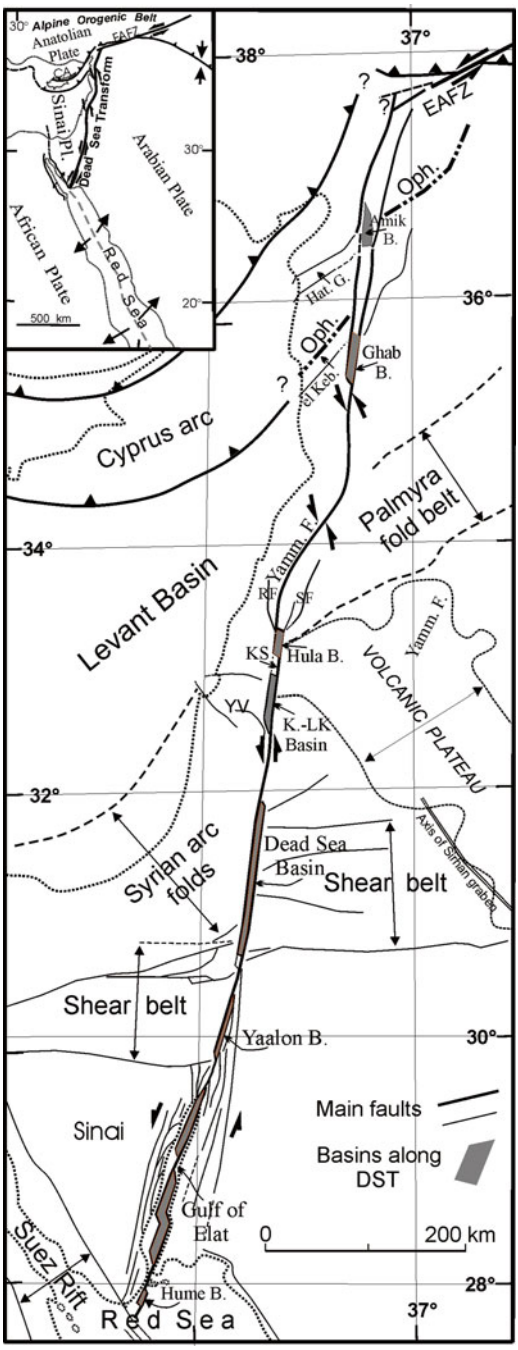

Fig. 5.1 The DST and its regional setting (*inset*). *EAFZ* East Anatolian fault zone, *K.-LK Basin* Kinnarot-Lake Kinneret Basin, *KS* Korazim saddle, *RF* Roum fault, *SF* Serghaya fault, *YV* Yizreel valley. Only main volcanic field is shown

the DST formed. In the Late Cretaceous plate convergence began along the junction of the Arabian platform and the adjacent basins with the Alpine orogenic belt (Şengör and Yilmaz 1981; Le Pichon et al. 1988; Yilmaz 1993) and the Syrian arc compressional structures formed on the platform next to parts of the future DST (Fig. 5.1, Garfunkel 1988; Brew et al. 2001a; Guiraud et al. 2001). This deformation ended when the DST formed. The DST cuts across all the older structures and its formation and development were accompanied by regional-scale uplifting and volcanism.

5.3 The Kinematic Framework

The DST is a prominent geologic discontinuity: the rock sequences and structures facing each other on its two sides are quite different. This is considered to be a result of a left lateral offset of ca. 100 km because its restoration matches all known geologic features across the southern DST, as far north as southernmost Lebanon (Quennell 1959; Freund 1965; Freund et al. 1970; Druckman 1974; Bandel 1981; Bandel and Khouri 1981; Segev 1984; Sneh and Weinberger 2003). The matched features include basement rocks, the facies belts and isopachs of the entire Cambrian to Late Cretaceous sedimentary cover, the lines along which the regional Early Cretaceous erosion truncated older stratigraphic units, as well as the narrow lineaments (belts of faulting and strong folding) of the Central Negev-Sinai shear belt (southern part of the Syrian arc, Fig. 5.1). The latter trend at large angles to the DST, so their matching gives the best estimate of the offset along the DST – ca. 105 km in the Dead Sea area (Fig. 5.1, Quennell 1959; Bartov 1974; Garfunkel 1981). The patterns of magnetic anomalies in Jordan and Israel are also displaced ca. 105 km (Hatcher et al. 1981). Shaliv (1991) noted that the Yizreel Valley could be matched with the Sirhan depression (Fig. 5.1). However, while the latter subsided markedly in the Late Cretaceous (Basha 1982), activity of that age along the Yizreel Valley was not documented. They should have connected beneath the volcanics of the Golan Heights, but such a connecting structure was not observed (Shulman et al. 2004; Meiler et al. 2011), so the significance of this correlation requires further study.

Farther north in Lebanon the DST marks a discontinuity between the mid-Cretaceous carbonate series on its two sides (Saint-Marc 1974; Walley 1998), but an offset marker – the front of ophiolite and related nappes – is known still farther north, near the Syria-Turkey border (Fig. 5.1). These nappes were thrust over the Arabian platform in the Late Cretaceous, and now are intercalated between within the sedimentary section (Ponikarov 1964; Ponikarov et al. 1969; Kopp and Leonov 2000). Their absence in the section 3–10 km SE of their exposures tightly constrains the end-Cretaceous position of their front (it may have been defined by a fault zone: Ponikarov et al. 1969, Figs. 5.1 and 5.6). Matching the ophiolite nappe front across the DST reveals a left lateral offset of 65–70 km (Freund et al. 1970; Al-Maleh et al. 1992; Westaway (2003) favored an offset of 55 km). This is supported by the distribution of Early Miocene marine beds filling a depression SE of the ophiolite nappes (Ponikarov 1964; Ponikarov et al. 1969; Krasheninnikov 2005,

see 5.3, 5.5.2.3). An offset of only 20–25 km, as suggested by Trifonov et al. (1991) is unlikely, because when restored this leaves notable bend of the original nappe front where it crossed the future DST. The difference between this estimate and the offset farther south will be discussed below see (5.5.2.4).

The motion along the DST is independently constrained by the regional plate kinematics because it takes up most of the Africa-Arabia plate separation, i.e. the Red Sea opening (Dubertret 1932; Freund 1965, 1970; McKenzie et al. 1970; Le Pichon et al. 1973). Taking into account the relatively small opening of the Suez rift and the stretching of the Red Sea margins, a left-lateral offset of 100–110 km is inferred along the DST, i.e. the Sinai-Arabia plate boundary (Freund 1970; Joffe and Garfunkel 1987). Within error, this is the same as the offset deduced from the geology along the southern half of the DST, though the geometry of the Red Sea opening is deduced from completely independent data. The Sinai-Arabia Euler pole of the motion of these plates, i.e. the DST motion, is estimated to be located in NE Libya or the nearby part of the Mediterranean (Quennell 1959; Freund 1970; Garfunkel 1981). Such a position of the Sinai-Arabia pole implies transtension along the south of the DST and transpression along its northern part (Fig. 5.1). This pole is close to the Arabia-Africa Euler pole (i.e. the Red Sea opening) because these motions are similar. Integration of all these constraints allows to derive well constrained plate kinematic models (e.g. Joffe and Garfunkel 1987; Le Pichon and Gaulier 1988; and see Sect. 5.4).

5.4 The Chronological Framework – The History of Motion

Several observations constrain the history of motion along the DST. It postdates the ca. 20–24 Ma old swarm of Red Sea dikes, as the northern dikes experienced the entire lateral offset (Fig. 5.3, Eyal et al. 1981; Steinitz et al. 1981; Steinitz and Bartov 1991). The ages of the oldest fills of basins along the DST also constrain the time of the beginning of the motion, because the basins resulted from the lateral motion (Garfunkel 1981; Garfunkel and Ben-Avraham 2001, see Sect. 5.5). Drillholes in the Dead Sea basin reached palynologically dated Early Miocene sections (Horowitz 1987) that are considerably thicker than coeval sections (Hazeva Formation) on the western basin flank, indicating that the basin existed already at that time (Garfunkel and Ben-Avraham 1996, 2001). Near Tiberias basalt flows with K-Ar ages of 17 ± 3 Ma to ca. 15.5 Ma occur in the middle of the sediment fill of a small marginal basin (Tiberias sub-basin), while ca. 20 km farther south its entire fill consists of basalts, the oldest ones having K-Ar ages of ca. 15.5 Ma (Shaliv 1991). The nearby 4.25 km deep Zemah 1 well (Z in Fig. 5.5, just south of Lake Kinneret) in the main basin along the DST bottomed in Middle Miocene beds (Horowitz 1987) which are >1 km above the base of the ca. 5 km thick fill (Ben-Avraham et al. 1996). Thus, in this area basins formed already at the beginning of the Middle Miocene or somewhat earlier. Moreover, this part of the DST was a structural boundary already at that time, because in the area that originally was

located east of it no basin formed and volcanism was very restricted (Garfunkel 1989; Weinberger et al. 2003), and the early faulting west of the DST did not extend east of it (see below). Evidence from the Sinai triple junction, at the south of the DST, also indicates its early Miocene activity (see Sect. 5.5.1.1).

Along the northern part of the DST marine Early Miocene sediments are preserved in a depression SE of the ophiolite nappes (Ponikarov 1964; Ponikarov et al. 1969; Kopp and Leonov 2000; Krasheninnikov 2005; Hardenberg and Robertson 2007). These works show that west of the DST the Nahr el-Kebir (Latakiye) depression (Figs. 5.1 and 5.6) formed in the Aquitanian, shortly before initiation of the DST in the south, and was accentuated as a graben in the Middle Miocene. In its SW part ca. 1.7 km thick marine sediments accumulated by the end of the Miocene (may be less farther NE). Restoring the DST offset as estimated above aligns these beds with an area east of the DST where Early Miocene sections reach a combined thickness of ca. 0.7 km, which most likely record the eastward extension of the depression west of the DST. Here a Middle Miocene graben is not apparent, but the sediments of this age are folded on NE-SW trending axes, while west of the DST such folds are absent. These features show that here the two sides of DST were deformed differently, which suggests that it was active and formed a structural discontinuity already in the Middle Miocene.

These lines of evidence constrain the beginning of lateral motion along DST to between 20 Ma and ca. 17–16 Ma ago. This is considerably younger than the initial breakaway of Arabia from Africa along the Red Sea-Suez rift line, but is close to the time when faulting along the Suez rift was reduced, seafloor spreading began in the Gulf of Aden, and the Arabia-Africa plate separation accelerated (Garfunkel and Bartov 1977; Bosworth 2005; Garfunkel and Beyth 2006, and references therein). These events are interpreted to show that at that time most of Arabia-Africa motion north of the Red Sea was transferred to the DST. Avni et al. (2012) raised the possibility that earlier faulting without lateral offset occurred along the DST, based on analysis of ancient landscape. Though quite possible, this requires further study.

During the very early stage of the DST lateral motion some right lateral motion may have continued on the Central Negev-Sinai shear belt lineaments (Fig. 5.1, Calvo 2002), but the interaction between these structures and the DST requires further study. However, they need not have obstructed each other, similar to the present situation in southern California where active transverse faults meet the San Andreas Fault (Jennings 1973).

Another constraint on the DST slip history is provided by magnetic anomalies that record seafloor spreading, i.e. Africa-Arabia plate separation, since 5–3 Ma ago in the southern and central Red Sea (Roeser 1975; Chu and Gordon 1998). With plausible Euler poles for the Red Sea opening this translates to 40 ± 2 km of oblique opening near its northern end. Opening of the Suez rift in the last 5 Ma may have taken up ca. 5 km, leaving a lateral slip of about 33–37 km (average rate of 6.5–7 mm/year) along the DST, which is 30–35 % of the total offset. Thus the Miocene motion amounted to ca. 2/3 of the total lateral DST offset.

GPS studies of the present plate motions (Reilinger et al. 2006; Le Beon et al. 2008; ArRajehi et al. 2010; Le Pichon and Kreemer 2010; Al Tarazi et al. 2011; Reilinger and McClusky 2011) found a slip rate of ca. 4.0 to 5.5 mm/year along the DST, compatible with the slip rates indicated by up 50–100 kyr old markers (Garfunkel 2011), but they do not resolve well the much smaller transverse component of motion. These results suggest that the present slip is slower than the average rate in the last 5 Ma. Alchalbi et al. (2010) found a slip rate of 1.8–3.3 mm/year in NW Syria, slower than found in previous studies, but compatible with the evidence that there the total offset was less than farther south.

The constraint from the southern Red Sea provides a datum that can be used for dividing the Sinai-Arabia plate motion into two periods – before and after 5 Ma ago (Garfunkel 1981; Joffe and Garfunkel 1987). This does not imply a discontinuity in motion (as suggested e.g. by Hempton 1987), which is contradicted by the evidence from the Gulf of Aden and the Red Sea showing that plate motions were continuous and quite uniform (Le Pichon and Gaulier 1988; Garfunkel and Beyth 2006 and references therein). Nor does it imply a sudden change of motion at that time or that plate motions were uniform in the two periods. The major young structures along the southern half of the DST (flanked by rigid plates) existed for some time (see Sect. 5.5.1) so they can be used to constrain the geometry of motion during the younger period. Combining their geometry with the above constraint on the amount of motion, allows estimating the entire motion during the last 5 Ma as ca. 1.45° about an Euler pole at 32.8°N, 22.6°E (uncertainty ca. 1°). However, using this pole to reconstruct the total DST motion would produce overlaps of the plate edges, which indicates that the pole position changed. The total pre-5 Ma motion is estimated as ca. 2.7° about a pole located some 4° farther west, which involves a change in the direction of motion of up to ca. 10° along the southern DST (Joffe and Garfunkel 1987). The GPS data seem to imply a continuing eastward shift of the Euler pole and a slight slowing of the slip rate. Reilinger et al. (2006) suggested a present day Euler pole at 32.8°N, 28.4°E (± ca. 3.5 °) for the DST, but this leads (given the Red Sea opening) to problematic inferences regarding the Suez rift (Garfunkel 2011). Westaway (2003) proposed an Euler pole at 31.1°N, 26.7°E, and a motion rate of 0.434°/Ma. This implies a northward increasing slip rate, in conflict with the GPS data (Reilinger et al. 2006; Reilinger and McClusky 2011; Alchalbi et al. 2010), so this model needs revision.

Le Pichon and Kreemer (2010) analyzed the GPS data of the Eastern Mediterranean region. Their results are compatible with the above estimates, though they do not resolve the present Africa-Sinai motion. Most important, their results and those of (Reilinger et al. 2006) reveal an overall rotation of the region surrounding the DST relative to Europe about an Euler pole at the north of the Nile Delta. This profound insight has important implications regarding the regional plate motions, but since this applies to a scale this is outside the scope of the present work.

In summary, the foregoing account shows that the plate kinematic setting of the DST, known is general outline, provides a framework of integrating data from its various parts, but refinement of the present models is still desirable.

5.5 Shallow Structure of the Dead Sea Transform

The DST is not a perfect small circle in map view, so its lateral motion inevitably produces misfits between the edges of the bordering plates, which cause local transtension or transpression (Figs. 5.1 and 5.2, Quennell 1959; Garfunkel 1981). This produces a variety of secondary structures, similar to those found along other major strike slip fault zones (Crowell 1974; Mann et al. 1983; Şengör et al. 1985; Harding et al. 1985). Transtension arises where the major strike slip fault line bends or steps in the same sense as the fault slip (releasing bend). This produces rhombic depressions – pull-apart basins (rhomb grabens) – that grow by becoming longer, so their length cannot be less than the lateral offset during their development (Fig. 5.2a). Thus, when the slip rate is known, the lengths of pull-apart basins put constraints on their ages. Their growth also increases the area enclosed by the bordering plates (Fig. 5.2b). Where major strike slip faults bend or step opposite to the sense of slip (restraining bends), transpression arises, which will produce folds, thrusts, or horsts. Such secondary structures appear all along the DST. The larger secondary structures are well over 10 km long and thus developed over several million years, so the pattern of major faults delimiting them must have persisted over these time intervals. The major faults are actually zones of much fracturing, several hundred meters wide, and along them much shorter structures (1 km to tens of meters long) are developed. Their small size suggests growth in short periods, probably much shorter

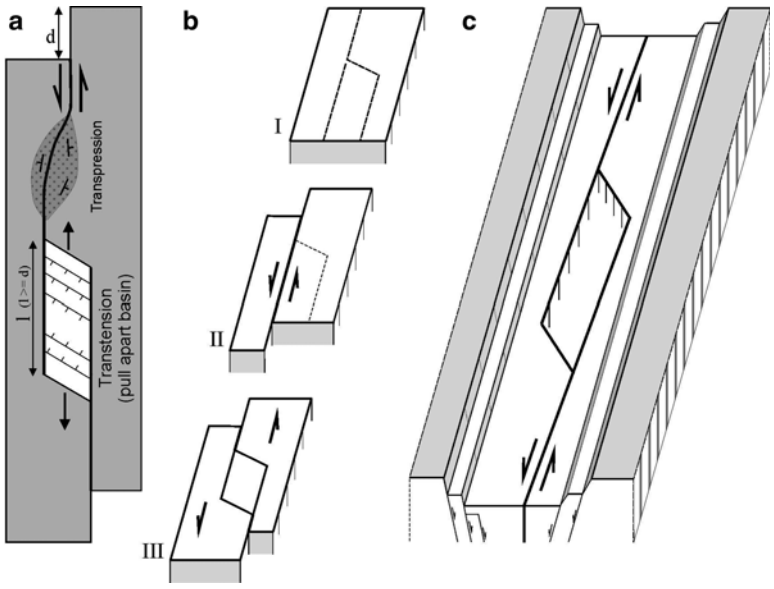

Fig. 5.2 Secondary structures along the DST. (**a**) conditions for transtension and transpression.; (**b**) Increase in are during pull-apart formation. (**c**) structural relations along southern (transtensional) part of DST (See text for discussion)

than 1 Ma, which points at rearrangement of the fractures on which the slip along the fault zones occurred at any given time.

In what follows only the larger secondary structures will be examined. Because of the position Euler pole of the DST, transtension or transpression dominate along its southern and northern parts, respectively (Fig. 5.1), so they will be treated separately.

5.5.1 Southern Part of the Dead Sea Transform

This part of the DST, south of Lebanon, is mostly marked by a prominent 5–20 km wide valley (transform valley), mostly with uplifted flanks, in which all or most of the lateral motion takes place. The valley floor is largely covered by very young sediments, so the deeper structure is inferred from drilling and geophysical data. Along the valley the most conspicuous structures are longitudinal faults of two types (Garfunkel 1981; Garfunkel and Ben-Avraham 2001, Fig. 5.2c): (a) normal faults that extend along most of the valley margins, and (b) left stepping strike slip or oblique slip faults within the valley that delimit a string of pull-apart basins. Also present are faults extending across the transform valley. Recent reviews (Ben-Avraham et al. 2008, 2012) summarize many geophysical data along this part of the DST, focusing on the subsurface. Below is an updated review of the structure in the upper crust integrating a wider set of geological and subsurface data and relating it to the lateral offset.

5.5.1.1 The Sinai Triple Junction Area

The southernmost part of the DST is now marked by the ca. 30 km long Hume Deep pull-apart basin (Fig. 5.3a, Ben-Avraham et al. 1979). It is separated from the Gulf of Elat (‘Aqaba) by the Tiran strait saddle formed by transpression, east of which reef terraces on the Tiran Island, probably <2 Ma old, were uplifted up to ca. 500 m above sea level (Garfunkel 1981; Goldberg and Beyth 1991). In the SW the NNE-SSW trending DST structures are cut off near the northern extremity of the Red Sea axial depression by the NW-SE trending faults that characterize the entire width of the Red Sea basin and the Suez rift (Cochran 1983, 2005; Garfunkel 1987; Gaulier et al. 1988; Mart and Hall 1984). Moreover, while the Bouguer anomaly over the Hume Deep pull-apart is strongly negative, like over the other pull-apart basins along the DST, a positive Bouguer anomaly characterizes the Red Sea basin (Ben-Avraham et al. 1979; Ben-Avraham 1985; Cochran 2005). This reflects the transition to a crust that was shaped by plate separation rather than in a strike-slip regime.

The early stages of the DST history in this area are recorded by the very early and younger Miocene marine sediments, 0.5–1 km thick known in Midyan and on the southern tip of Sinai (Fig. 5.3a, Dullo et al. 1983; Garfunkel 1987; Cole et al. 1995;

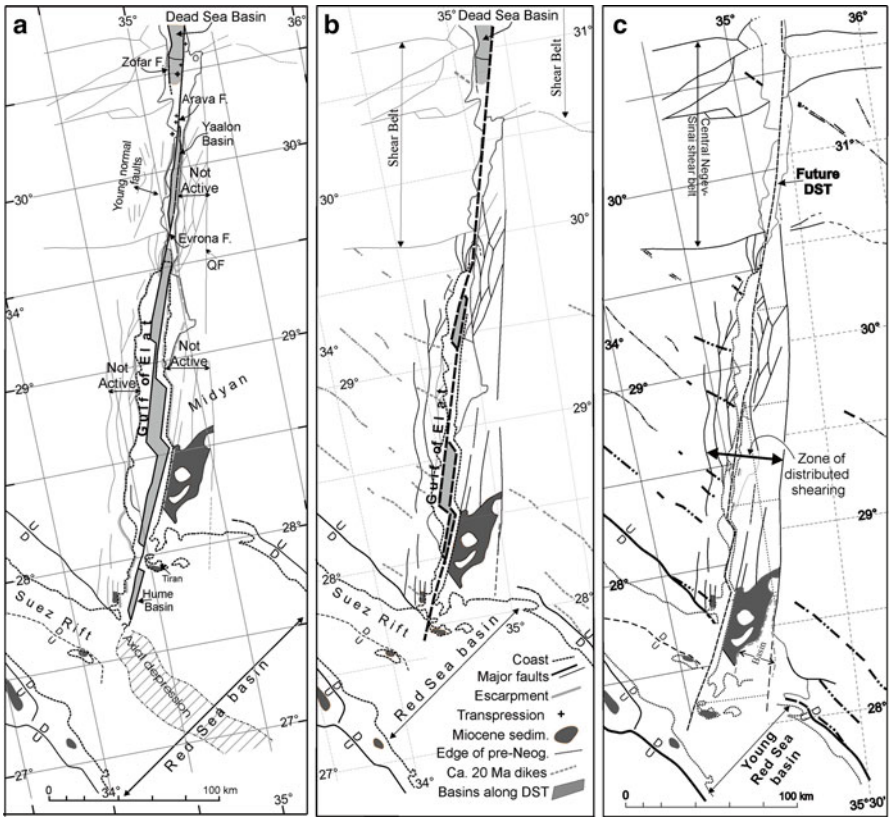

Fig. 5.3 The southern part of the DST. (**a**) present situation. (**b**): reconstruction of 40 km lateral offset (close to end Miocene). (**c**) Reconstruction of the entire transform offset. Abbreviations: *QF* el Quweira faults, *ZF* Zofar fault

Hughes et al. 1999). These beds cover the southern ends of belts of strike-slip faults along the two sides of the Gulf of Elat that were active in the Miocene (further discussed in Sect. 5.5.1.2), and fill a depression in Midyan. Restoration of the lateral motion (Fig. 5.3c) eliminates the Gulf of Elat (between these fault belts) and also aligns the uplifted edges of Sinai and NW Arabia, which shows that before formation of the DST they formed a continuous fault-controlled margin of the very young Red Sea-Suez basin. When the DST formed this margin was breached by a ca. 50 km wide belt of NNE-SSW trending strike slip faults. The above mentioned Miocene beds formed in a marine embayment over the southern part of this belt, so their age constrains the inception of the DST to the Early Miocene. The most subsiding area in Midyan (up to >2 km of sediments) was located 20–30 km east of the break that developed into the Gulf of Elat, but it did not extend much to the north. The later history of these features is treated below (Sect. 5.5.1.2).

5.5.1.2 The Gulf of Elat ('Aqaba) Segment

This segment comprises the ca. 180 km long depression under the Gulf and also the fault belts along its uplifted margins (Fig. 5.3a). The faults in these belts displace left laterally the ca. 20 Ma old Red Sea dikes, proving that they belong to the DST system (Eyal et al. 1981). Lateral offsets of individual faults range from ca. 1 km to >10 km (Eyal et al. 1981); the largest offset, ca. 20 km, probably occurred on the Al-Quweira Fault in SW Jordan (Segev 1984). The total offset reached 40–50 km. Pre-transform sediments and continental Miocene beds are preserved in small pull-aparts along these faults, which proves that faulting occurred before the sediment cover was eroded from the higher standing areas next to these depressions. On the other hand, strike slip faults that extend to the Gulf are truncated by normal faults along its coast, while inland some faults are truncated by an erosion surface or overstepped by (undated) continental sediments. In Midyan the younger Miocene beds are not visibly displaced by the marginal strike-slip faults. These features indicate that the strike slip faults along the Gulf flanks were active early in the DST history and then the lateral motion was distributed in a wide zone, but later (late in the Miocene?) they became inactive and the lateral motion was concentrated along the depression occupied by the Gulf of Elat ('Aqaba).

The Gulf is delimited on both sides by active normal faults that extend close to its coasts (not shown on Fig. 5.3a for clarity). Within the Gulf three large pull-aparts, well expressed in the bathymetry, are developed between major longitudinal left-stepping strike slip faults (Fig. 5.3a, Ben-Avraham et al. 1979; Ben-Avraham and Garfunkel 1986; Ben-Avraham et al. 2008, 2012). The upper ca. 1 km of the sediment fill, imaged by seismic reflection, records continuing, downward increasing, syn-depositional deformation (tilting, faulting, and in the south also arching), but as the age of the sediments is not constrained, detailed interpretation of the deformation history (e.g. Ehrhardt et al. 2005) are very doubtful. Several narrow ridges in the southern pull-apart may express diapirs of Miocene evaporites (Ben-Avraham et al. 1979) that probably formed next to the Miocene low of Midyan.

Given the lateral offset accommodated in the marginal shear zones, the lateral offset within the Gulf hardly amounted to ca. 2/3 of the total offset. The lengths of the pull-aparts (ca. 40 km, 35 km and 60 km, from north to south) show that they could accommodate only a part of the total DST offset (see Fig. 5.2). This suggests that they formed some time after initiation of the DST, which is supported by reconstruction of part of the motion (Fig. 5.3b). A negative Bouguer anomaly, up to ca. −100 mgal over the pull-aparts (Ben-Avraham 1985), indicates ≥5 km thick sediment fills. However, the negative anomaly extends also over the relatively shallow part of the Gulf west of the southern pull-apart, indicating that a thick sediment fill exists beneath this area as well. This is interpreted as showing that this area was part of a subsiding pull-apart earlier in the evolution of the Gulf, which is supported by the reconstruction of part of the motion (Fig. 5.3b).

Thus, initially the lateral motion along the southernmost part of the DST was distributed over a wide belt of closely spaced strike slip faults that extended in the

north to the central Negev-Sinai shear belt (Fig 5.3c). Later, in the late Miocene (?), lateral motion became concentrated in the middle of this belt where the Gulf of Elat depression developed, while the faults along its margins became inactive. As the active faults along the Gulf lead to transtension (Garfunkel 1981), which is not seen along the marginal strike slip fault zones, this history appears to express increasing separation of the flanking plate edges along this part of the DST, which can be related to eastward shifting of the Sinai-Arabia Euler pole (Garfunkel 1981, see Sect. 5.4).

5.5.1.3 The Southern and Central Arava Valley (Wadi Araba) Segment

This segment extends from the Gulf of Elat to the Dead Sea basin (Fig. 5.3a, Garfunkel et al. 1981; Bartov 1994; Ten Brink et al. 1999; Frieslander 2000; Avni et al. 2000; Calvo 2002). In the south, it is separated from the onland northern end of the Gulf of Elat depression by a weakly transpressional structural saddle that is crossed obliquely by the Evrona Fault. North of it the little studied Yaalon basin pull-apart, marked by a ca. 60 km long negative gravity anomaly, is developed between the left stepping Evrona Fault and Arava Fault (Fig. 5.3a). Its southern half, 5–6 km wide, is expressed by a land-locked depression that records continuing subsidence. Farther north the basin narrows to 2–3 km and has no topographic expression, so it is not clear whether it still subsides. The subsurface distribution of Cretaceous beds revealed by drilling in the middle part of the basin indicates a ca. 40 km left lateral offset along its western border fault, so the rest of the lateral motion must have taken place farther east (Bartov 1994).

North of the Yaalon basin exposures of the pre-transform series of the western DST flank extend eastwards as far as the Arava Fault (Frieslander 2000), forming a ca. 20 km long structural saddle between the Yaalon basin and a ca. 8–9 km wide graben farther north that is delimited by the Arava Fault on the east and the Zofar Fault on the west (Fig. 5.3a, Bartov 1994; Bartov et al. 1998; Calvo 2002). This graben is filled by a few kilometers of Miocene continental beds (Hazeva Formation). Seismic data show that the pre-transform series beneath this fill, to a distance of at least 35 km north of the Yaalon basin, is the same as that of the western DST flank, but differs markedly from that exposed a short distance east of the Arava fault (Frieslander 2000; Ryberg et al. 2007). The juxtaposition of different sections across the Arava fault indicates a large lateral offset along this fault.

Originally the graben between the Arava and Zofar Faults extended to the northern Arava. There it continued to subside and became a part of the Dead Sea basin, but its part south of the transverse Buwirida Fault ceased to subside and was tilted westward, probably during a phase of local transpression, exposing ca. 2 km of its Miocene fill (Fig. 5.3, Bartov 1994; Calvo 2002). The age of this event is constrained to the late Miocene or somewhat later, as it postdates the eroded Miocene beds (Hazeva Formation) but predates the hardly disturbed unconformably overlying Pliocene fluviatile beds (Arava Conglomerate; Avni et al. 2000). A few other transpressional structures are developed in this area (Fig. 5.3b, Garfunkel et al.

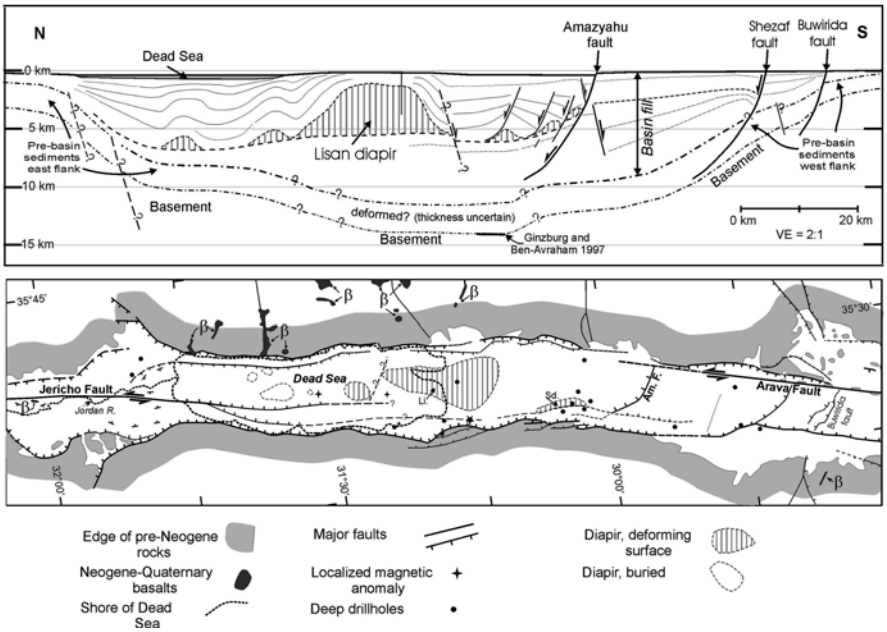

Fig. 5.4 The Dead Sea basin. *Top*: Cross section along basin axis. *Bottom*: main structural features. *Li* Lisan Diapir, *Sd.* Mount Sedom diapir

1981; Galli 1999). A related observation is that in (Early?) Pliocene times a stream originating in the eastern DST flank – the Edom river – flowed across this part of the central Arava Valley and transported characteristic pebbles to the Negev (Ginat and Avni 1994), probably signifying a period of local uplift, due to transpression, of this part of the Arava Valley.

The tectonic situation changed in Late Pliocene-Quaternary times, leading to formation of the present topographic low position of the Arava Valley. This is evidenced by the development at that time of a series of NNE-SSW to N-S striking normal faults (sometimes with a minor left lateral component) in a ca. 30 km wide belt west of the northern Yaalon basin and of the more northern part of the Arava Valley (Fig. 5.3a, Avni et al. 1994). These faults are believed to record a young increase of transtension along the southern part of the DST, resulting from an eastward shift of the Euler pole, as discussed above (Sect. 5.4).

5.5.1.4 The Dead Sea Pull-Apart Basin

The Dead Sea basin, ca. 150 km long, formed between the left stepping left lateral Arava Fault and Jericho Fault (Fig. 5.4, Quennell 1959; Garfunkel 1981; Garfunkel and Ben-Avraham 1996, 2001; Ben-Avraham et al. 2008, 2012). It is topographically well expressed and is also outlined by a conspicuous negative Bouguer anomaly gravity which records the extent of the thick basin fill (Ten Brink et al. 1993). It

is the longest pull-apart basin along the DST and the only one that is longer than its total lateral offset. The basin began to subside already in the Early Miocene (>16 Ma), as noted above (see 5.4). Data from outcrops and wells show that the basin fill comprises three divisions: Miocene silici-clastics (Hazeva Formation); latest Miocene-early Pliocene evaporites, mainly halite (Sedom Formation); post-evaporitic lacustrine and fluvial sediments, mainly clastics (Kashai and Crocker 1987; Horowitz 1987; Gardosh et al. 1997; Garfunkel and Ben-Avraham 2001; and references therein).

Available seismic reflection and well data (Neev and Hall 1979; Kashai and Crocker 1987; Ten Brink and Ben-Avraham 1989; Garfunkel and Ben-Avraham 1996; Al-Zoubi and ten-Brink 2002; Larsen et al. 2002; Ginzburg et al. 2006; Ben-Avraham et al. 2008, 2012) allow an updated interpretation of the basin structure (Fig. 5.4). They show that it is dominated by an 8–10 km wide central trough that formed between the extensions of the Arava and Jericho faults, in which the lateral motion takes place. It is separated from the uplifted and little deformed transform shoulders by marginal blocks, wider on the western side. Several transverse faults extend across the basin. The fill of the central trough thickens northward from a few km in the central Arava Valley to ca. 12 km near the transverse Amatzyahu Fault (Khunayzira Fault). Farther north, south of the Lisan diapir, the top of the basement is 13–14 km deep (Ginzburg and Ben-Avraham 1997). These figures are compatible with recent seismic refraction data (Ten Brink et al. 2006; Mechie et al. 2009; ten Brink and Flores 2012). North of the Amatzyahu Fault the base of the evaporite series is at a depth of 3–3.5 km and deepens to 6 km northward (Ginzburg et al. 2006). As here the pre-transform series is at most ca.3 km thick – its thickness on the adjacent western basin margin – the pre-evaporite Hazeva Formation is inferred to be 5–7 km thick. This is much more than in boreholes near the basin margins, implying great early subsidence of the central trough.

The evaporitic series is present only north of the Amatzyahu Fault (Khunayzira Fault) where post-Hazeva subsidence was greatest. It was deposited over a short time interval, perhaps no longer than 2–3 Ma (Zak 1967). The original thickness, probably reaching ca. 2 km, was modified by the growth of the Sedom diapir, Lisan diapir, and smaller disapirs (Fig. 5.4). Superimposed on the northern part of this area is the box-shaped depression now occupied by the waters of the Dead Sea, which defines the extent of the greatest young subsidence that could not yet be filled by sediments.

The available seismic reflection profiles do not reveal much deformation of the basin fill. Broad roll-overs are seen north of the Shezaf Fault and Amatzyahu Fault (Khunayzira Fault) (Fig. 5.4b), suggesting that these faults are listric, but this cannot be resolved from the published seismic data. Smaller scale deformation is not discernible, though considerable deformation is expected beneath the basin (see Sect. 5.5.1.7).

The deep structure of the northern part of the basin, now under the waters of the Dead Sea, is hardly known. A seismic refraction line along its western side records a basement depth of 5.5–7 km (Ginzburg and Ben-Avraham 1997), but this probably represents the marginal blocks where the basement is expected to be 5–6 km deep according to the En Gadi 2 well (Fig. 5.4). The Bouguer anomaly over the central trough is much more negative than along the seismic profile, suggesting a thicker fill

and thus a considerably deeper basement. On the other hand, 2–3 km north of the Dead Sea the basement is only ca. 3 km deep and shallows northward according to seismic and borehole data (Lazar et al. 2006; Al-Zoubi et al. 2007). How the basement depth changes it is not known. The data from north of the Dead Sea further show that there the pre-transform sedimentary sequence of the eastern DST flank extends beneath the Jordan Valley as far west as the Jericho Fault. Moreover, farther south the magnetic anomaly of the eastern basin flank extends over the Dead Sea, whereas the anomalies of the western flank are truncated along the marginal step (Frieslander and Ben-Avraham 1989). This shows that the Jericho Fault accommodated the entire lateral transform offset, and also that considerable lateral motion occurred on its southward continuation along the western side of the central trough, probably at least as far south as the site of strong deformation at ca. lat 31°16′ (shown as star in Fig. 5.4, Bartov and Sagy 2004).

The growth of the Dead Sea basin was accompanied by igneous activity on its flanks. Along the eastern margin 9–5 Ma old basalt flows and younger small vents and flows are present (Steinitz and Bartov 1991). West of its southern part a 6.4 Ma old dike and a nearby vent are present. In addition, a short-wavelength magnetic anomalies north of the Lisan diapir (Frieslander and Ben-Avraham 1989) most likely record small igneous bodies inside the basin.

5.5.1.5 The Southern Jordan Valley

This little studied segment (Fig. 5.4) extends to ca. 70 km north of the Dead Sea where it narrows to < 4 km at the Bet Shean saddle. Its young fill is much thinner than in the Dead Sea according to gravity anomalies (Ten Brink et al. 1999). The southern part of the Jericho Fault, which extends along the valley floor, records transpression (Garfunkel 1981; Rotstein and Bartov 1989; Gardosh et al. 1990). Ca. 25 km north of the Dead Sea the Zahrat el-Qurein (Grain Sabt) half dome next to the Jericho Fault (Fig. 5.4) exposes ca. 350 m of tilted Miocene (?) coarse clastics (base not seen), unconformably overlain by a basalt flow and by young Quaternary sediments (Bender 1974). The basalt records magma ascent along the DST trace. The margins of the southern Jordan Valley are controlled by normal faults. In the east they trend close to N-S, but in the west their trends are variable, and some branch into the western flank of the valley (Fig. 5.4).

5.5.1.6 The Central and Northern Jordan Valley

This segment extends ca. 90 km north of the Bet Shean saddle to Lebanon. It comprises the Kinnarot-Lake Kinneret (Sea of Galilee) basin (Kinnarot-LK basin) the Korazim saddle, and the Hula basin (Fig. 5.5). It differs from the more southern segments by its more complex structure, by the occurrence of much igneous activity both along the DST and on its flanks, and by the considerable deformation of its western flank.

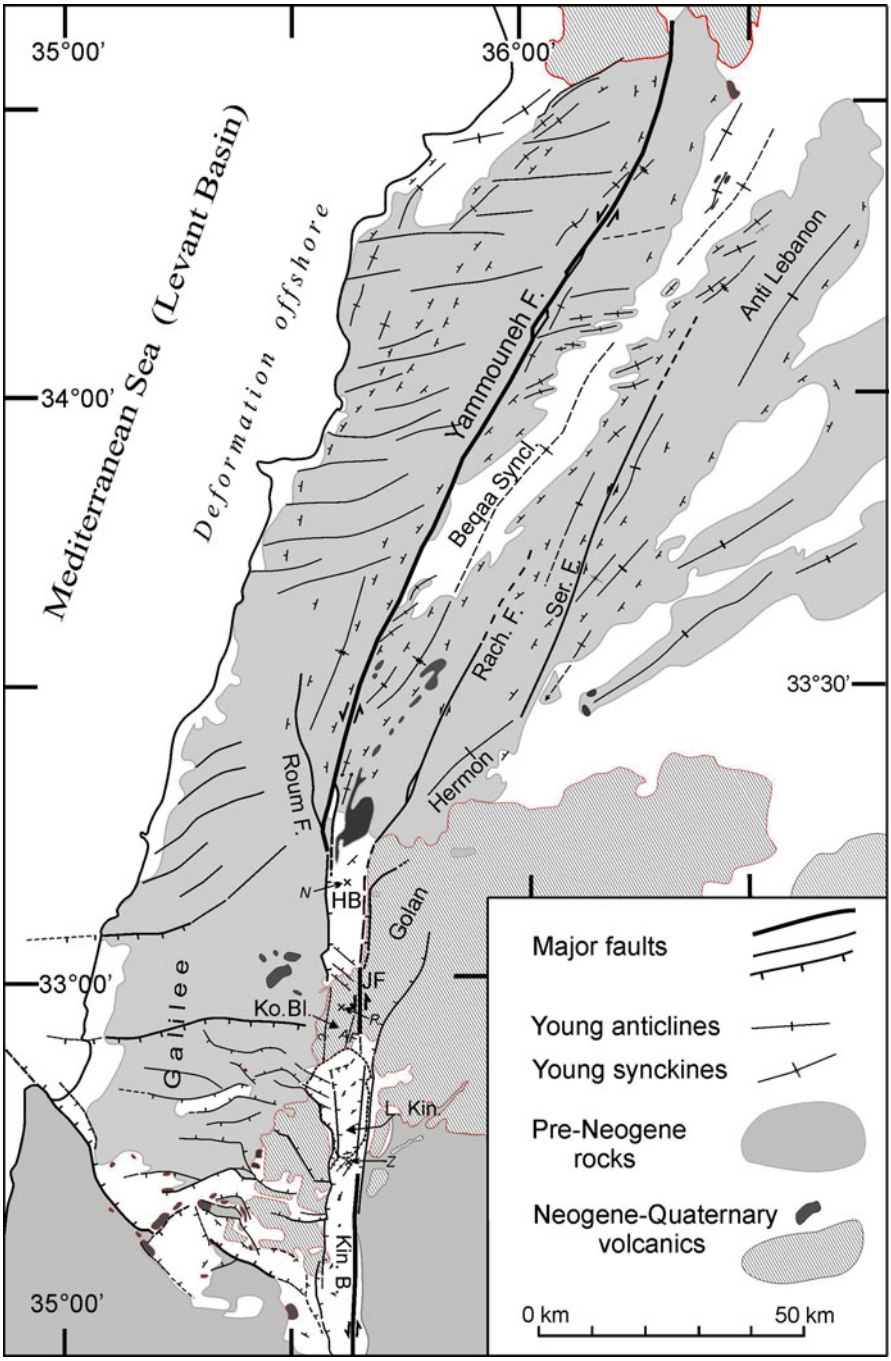

Fig. 5.5 The northern Jordan Valley and Lebanon segments of the DST. *AF* Almagor fault, *HB* Hula Basin, *JF* Jordan Gorge fault, *Ko. Bl.* Korazim block (saddle), *L. Kin.* Lake Kinneret, *Kin. B.* Kinnarot Basin, *R* Rosh Pina drillnole, *Rach. F.* Rachaya fault, *Ser. F.* Serghaya fault

Here the oldest exposed structure related to the DST is seen in a ca. 40 km long and up to 10 km wide low (also called the Tiberias sub-basin) on the western DST flank (Fig. 5.5). Its fill, up to 1 km thick, begins with 17–9 Ma old basalts (Lower Basalt) (see 5.4) interfingering with fluviatile-lacustrine sediments (Hordos Formation), together 400–750 m thick, overlain by continental and some marine sediments and volcanics, with ca. 5.2–4.0 Ma old flows (Cover Basalt) forming the top of the series (Schulman 1962; Shaliv 1991; Heimann et al. 1996).

Nearby the ca. 50 km long Kinnarot-LK basin formed along the main strand of the DST, with a ca. 5 km thick fill south of Lake Kinneret according to gravity data (Ben-Avraham et al. 1996). The 4.25 km deep Zemah 1 well (Fig. 5.5; Marcus and Slager 1986; Mittlefehldt and Slager 1986; Horowitz 1987) bottomed in Middle Miocene conglomerates (with basalt clasts), overlain by sediments that include Late Miocene and early Pliocene evaporites (980 m), mainly halite, which formed when an arm of the Mediterranean reached the DST from the west, and extended southward to the Dead Sea basin. The evaporites are intruded by gabbro sills (total thickness ca. 1.1 km), and are overlain by Pliocene volcanics broadly coeval with the Cover Basalt. The occurrence of igneous rocks, more voluminous than on the basin flanks, indicates preferential magma ascent along the DST. Seismic reflection data and mapping show that after extrusion of the Pliocene basalts the basin fill south of Lake Kinneret was deformed into broad folds with amplitudes reaching 1 km, and the fold crests were much eroded (locally down to the cover basalt), before being covered by a thin veneer of very young sediments. The deformation is interpreted as resulting from a young phase of transpression (Rotstein et al. 1992; Heimann and Braun 2000). In addition, very tightly folded Early Pleistocene beds were revealed in excavations at the Ubeidiya prehistoric site (Picard and Baida 1966), but the young cover obscures the extent of this type of folding.

In contrast, the more northern part of the Kinnarot-LK basin beneath Lake Kinneret subsided up to 2 km and was faulted in post-Cover Basalt times (Fig. 5.5, Ben-Avraham et al. 1996; Hurwitz et al. 2002; Reznikov et al. 2004). The main young structure is a graben, striking N-S, crossed by transverse faults, many of them ending up section. The part of the lake west of the graben is crossed by NW-SE striking faults that extend into the Galilee.

The Korazim saddle north of Lake Kinneret is separated from the basin under the lake by a major transverse fault zone (Fig. 5.5, Hurwitz et al. 2002). This saddle is underlain by a high standing block of pre-transform rocks (revealed by drilling) that is covered by 50–300 m of Neogene sediments overlain by 5.0–3.5 Ma old Cover Basalt, which in the north are covered by still younger flows that erupted through the plateau (Fleischer 1968; Horowitz 1973; Belitzky 1987; Heimann and Ron 1993; Weinstein 2012). Thus here too the DST served as a preferred path for magma ascent. The Korazim saddle is strongly faulted, with the fault blocks having rotated $11 \pm 4°$ ccw on vertical axes according to paleomagnetic data (Heimann and Ron 1993). On the east the Jordan Gorge Fault zone (Fig. 5.5, Garfunkel et al. 1981; Harash and Bar 1988) – the northward extension of the fault on the eastern side of the Kinnarot-LK basin – marks a prominent geologic discontinuity between the Korazim saddle and the Golan Heights (Michelson and Lipson-Benitah 1986).

Its straight trace and the lateral offset of historic and Holocene features (Ellenblum et al. 1998; Marco et al. 2005) show that this fault is the site of the ongoing lateral motion. Seismic reflection data show that it dips westward, indicating local transpression (Rotstein and Bartov 1989). The Almagor Fault west of the Jordan Gorge Fault (Fig. 5.5) is not continuous, so it could not accommodate much lateral motion, but is probably also active. The western boundary of the Korazim saddle is obscured by the Cover Basalt, but a fault with an irregular trace extends along this contact (Belitzky 1987). However, a structural discontinuity between the strongly deformed saddle and the less faulted western transform flank must extend along this boundary. The absence of a through-going fracture suggests there is no young lateral motion along this fault.

The Kinnarot-LK basin is difficult to interpret as a pull-apart, because it is not obviously related to left stepping strike slip faults. A critical point is that the pre-transform section under the Korazim saddle, penetrated by the Rosh Pinna 1 borehole, is offset ca. 50 km left laterally relative to the western DST flank (Freund et al. 1970; Hurwitz et al. 2002). Thus during a substantial part of the DST history lateral motion occurred along the western side of the Korzaim saddle, so originally the Kinnarot-LK basin could have developed as a pull-apart basin between left stepping faults: one west of the Korazim saddle and the other along the east side of the basin, the latter having extended southward to the Bet Shean saddle. At some stage this tectonic setting changed, as now lateral motion is identifiable only along the eastern side of the Korazim saddle. The young transpression south of Lake Kinneret probably formed during the tectonic change. The very young deformation under Lake Kinneret is probably linked to the coeval deformation of the Galilee (Hurwitz et al. 2002, see below).

The Hula basin, north of the Korazim saddle, formed between the left stepping Jordan Gorge fault and Yammouneh Fault, so it is interpreted as a pull-apart basin, (Fig. 5.5; Heimann and Ron 1993; Sneh and Weinberger 2003; Weinberger et al. 2009, 2011). The Notera 3 well (T.D. 2,781 m, Fig. 5.5) in the basin's center crossed a fill of sediments and basalt flows. At ca. 2,340 m a ca. 4.3 Ma old flow overlies an 8.8 ± 0.2 Ma old flow that, in turn, overlies red beds and interbedded basalts (base not reached) (Horowitz and Horowitz 1985; Heimann and Steinitz 1989). This shows that the present Hula basin subsided only since ca. 4.3 Ma ago, after a >4 Ma long period of no subsidence. Such a young age can be expected in view of its small length (ca. 15 km). The pre-ca. 9 Ma series is ca.1 km thick according to gravity data (Rybakov et al. 2003). Fault slivers near the NW corner of the Hula basin expose a strongly folded Late Miocene or older series, >400 m thick, of lacustrine beds and conglomerates built only of Eocene clasts (Kefar Giladi Formation; Glickson 1966; Sneh and Weinberger 2003; Weinberger et al. 2009). The structural setting in which these series formed was obliterated, but it probably differed from the present setting. The younger fill of the Hula basin fill is mostly flat, but in Pleistocene times a diagonal NE-SW striking fault associated with folding formed within the basin, while along its continuation NW of the basin several small uplifted structures formed (Schattner and Weinberger 2008; Heimann et al. 2009; Weinberger et al. 2009, 2011). These authors interpreted these structures as a result of young eastward shifting of the Euler pole, which caused southward expansion of the transpressive segment of the DST.

The area west of the central and northern Jordan Valley, including the Galilee, the Yizreel Valley (Esdarelon Valley), and the Tiberias sub-basin, is crossed by E-W, SSE-NNW, and NW-SE trending normal and oblique slip faults that formed while the DST was active. Here only a few major points can be mentioned. The trends of Middle Miocene faults in the Tiberias sub-basin and the Yizreel Valley form large angles with the DST (Shaliv 1991), but they do not extend east of it, which shows that at that time the DST was already a structural boundary. Paleomagnetic data reveal that the Miocene and Pliocene faulting west of the DST was accompanied by large rotations of the fault blocks about vertical axes, which led to overall E-W shortening and N-S extension of the Galilee (Ron et al. 1984). Since mid-Pliocene times ca. E-W trending normal faults dominated the structure of the southern half of the Galilee which led to N-S extension (Matmon et al. 2003). GPS data were interpreted by Sadeh et al. (2012) as showing that now the northern Galilee moves northward at a rate of 1 mm/year relative to the area south of the Yizreel Valley. Though close to the limit of resolution, this agrees with the structural evidence. The N-S extension (≥5 km) of the western DST flank decreases the lateral transform offset farther north. Some faults extend from the Galilee into Lake Kinneret (Fig. 5.5, Hurwitz et al. 2002). The resulting N-S extension due to these faults may have led to the young deformation and subsidence of Lake Kinneret, which is quite distinct from the transpression north and south of it.

The strong faulting of the western flank of this segment of the DST is considered to express its deformation when it moved laterally along the pronounced bend of the DST trace at the transition between its northern and southern parts. In contrast, only mild faulting affected the Golan Heights east of this segment of the DST (Fig. 5.5, Shulman et al. 2004; Meiler et al. 2011).

5.5.1.7 The Deformation Along the Southern Part of DST

The foregoing summary shows how the shallow structure along the DST was related to the plate kinemtics. It also reveals that most of the time and along most of the southern part of the DST the lateral motion and related deformation took place in an up to a few tens of kilometers wide zone. Only at the central Arava saddle and the Bet Shean saddle was the overall motion close to pure strike slip in narrow zones. Elsewhere the lateral motion took place in wide deformed zone, mainly on left stepping strike slip faults that deviate slightly clockwise from the overall transform. This produced varying amounts of transtension that led to the growth of a string of conspicuous pull-aparts (rhomb grabens) combined with normal faulting along the margins of the transform valley (Fig. 5.2c, Garfunkel 1981). Plate kinematic considerations and the structural history show that the transtension increased with time (see 5.4). This was achieved by structural rearrangements, well seen in the south, while in the Arava Valley and farther north by growth of pull apart basins combined with an increase in the role of the marginal normal faults.

The foregoing discussion focused on the shallow structures, but the features of these structures have also significant implications for processes at deeper level, especially when integrated with geophysical data. This topic is largely outside the scope of the present paper, but since such an analysis is rarely followed, a few points are presented below.

The deformation seen on the surface is expected to extend at least through the entire crust. This is supported by seismic data from the central Arava Valley which show that there the DST extends through the entire crust (Weber et al. 2004, 2009) and also by the difference between coeval volcanics across the DST near the Korazim plateau, which raises the possibility the DST motion affects the magma sources well below the Moho (Weinstein 2012). Here only a few implications of the shallow structures for the deeper deformation and some questions that they raise can be briefly discussed.

The most conspicuous deformation occurs during the growth of the pull-aparts. Most revealing are the data about the Dead Sea basin. As explained above, the southern part of the Dead Sea basin (in the Arava Valley) is floored by the continuation of its western flank, while in its northern part the eastern DST flank extends under the entire basin width (Fig. 5.4). Since the lateral offset along the DST moved these areas apart by ca. 105 km along the basin axis, the floor of the intervening part of the basin must have been stretched and thinned. This is confirmed by seismic and gravity data (ten Brink et al. 2006; Mechie et al. 2009) which show that the Moho under both the basin's center and it's flanks is at about the same depth – ca. 33 km. As the basin fill is up to 12–14 km thick, the crystalline crust under the middle part of the basin is only 22–20 km thick, compared with 30–32 km under the basin flanks. Similar arguments apply also to the deep Gulf of Elat and the Kinnarot-LK basins, where the Moho is not deeper than under their flanks according to gravity data, but there the crustal thinning is probably smaller than under the Dead Sea basin. Stretching of the floors of pull-aparts is expected also in view of the increase in area during their formation (Fig. 5.2b), and it also explains how the lateral slip along the pull-aparts is transferred from their SE to their NW extremities (Garfunkel and Ben-Avraham 1996, their Fig. 6).

Stretching of the crust under the basins should deform the basins' fills. The distribution of earthquake foci under the Dead Sea basin and their source mechanisms (Aldersons et al. 2003; Hofstetter et al. 2007, 2008) show that complex brittle deformation occurs beneath the entire basin width in both the upper and the lower crust, though the deformation pattern is difficult to infer. However, the structures known in the shallow parts of the basin fills (e.g. Gulf of Elat and Dead Sea) – transverse faults and downward increasing dips – probably can not account for the entire basins' growth, so this issue still requires further study.

If the crust beneath the major basins was modified only by stretching, then the basins would be strongly isostatically under-compensated because of the presence of a thick low-density of sediment fill. Exact local compensation of such narrow structures is not expected, but the continuing great subsidence of strongly under-compensated basins and the support of large deviations from isostatic equilibrium

are difficult to explain (cf. Ten Brink et al. 2006). However, the occurrence of igneous rocks along the DST (e.g. in the Zemah-1 well, the Zahret el-Qurein dome north of the Dead Sea, and the sources of the magnetic anomalies in its middle) and on its flanks raises the possibility that basalt intrusions in the stretched middle or even shallow crystalline crust contribute to decreasing the mass deficit. Noteworthily, seismic reflection studies (ten Brink et al. 2006; Mechie et al. 2009) show that beneath the middle of the Dead Sea basin material with upper crustal velocities forms a much smaller fraction of the crystalline crust than under the basin flanks. This is difficult to explain by mechanical stretching alone, but can arise if basic intrusions are emplaced into the lower velocity/lower density material of the upper half of the original crust. Underplating by igneous rocks was also inferred in the Imperial Valley, California, and the Baikal rift (Fuis et al. 1984; Nielsen and Thybo 2009).

Thinning of the crust beneath the basins would also influence the thermal regime. The thinned crust under the basins supplies less heat than the intact crust of their flanks, which should be taken into account while interpreting the data. As this is a shallow effect, it will be expressed in the heat flow after a period shorter than the DST history (in contrast to thermal effects originating well below the Moho). The heat flow of 38 mW/m^2 under the northern Dead Sea is similar or lower than that on its western flank (Ben-Avraham et al. 1978; Eckstein 1979; Schütz et al. 2012). In the northern Gulf of Elat the heat flow is 66 ± 30 mW/m^2, similar to 60.3 ± 3.4 mW/m^2 found east of 'Aqaba, and in Lake Kinneret it is 74 ± 4 mW/m^2, higher than in the Galilee (Ben-Avraham et al. 1978; Eckstein 1979; Förster et al. 2007). In these places the thinned crust contributes less to the heat flow at the surface than the intact crust under the transform shoulders. Thus, to account for the observed values, the heat flow from the mantle under the basins may well be higher than under their shoulders. On the other hand the occurrence of earthquakes in the lower crust under the basins (Aldersons et al. 2003) shows that the temperature there is low enough to allow earthquake generation (probably no more than 350–400 °C in the lower crust). More data and modeling of the thermal regime are required to integrate these considerations.

Pull-apart basin formation was also studied by finite element thermo-mechanical models that (Sobolev et al. 2005; Petrunin and Sobolev 2006) and by analogue modeling (e.g. Smit et al. 2010, 2011; Wu et al. 2009 and references therein). Though the models require further refinement to include the effects of lateral structural variations, changes of basin area, igneous activity, and changes of plate motions, they provide very important quantitative insights. However, as they apply to the entire crust and/or lithosphere, their discussion is outside the scope of this paper. Such models should eventually also yield insights into the structural changes that took place along the DST.

In summary, the foregoing considerations reveal how the shallow structures along the DST and their history are related to the motions of the flanking plates, and also show that combining the data regarding the shallow levels with geophysical data from deeper levels can provide insights that are otherwise very difficult to obtain.

5.5.2 *Northern Part of Dead Sea Transform*

The northern part of the DST differs from its southern part by having a sinuous trace and by the significant deformation of its flanks (Fig. 5.1) which is interpreted as expressing transpression. This part of the DST was less studied than the southern part, and its nature was much debated. Here an updated summary of the main available information and unresolved problems is attempted.

5.5.2.1 The Lebanon Restraining Segment

The conspicuous ca. 150 km long Yammouneh Fault extends along the east side of the Lebanon range, and is marked by a ca. 2 km wide damage zone in which much mesoscale fracturing, small scale folding, abundant horizontal slickensides, and small pull-aparts are developed (Heybroek 1942; Hancock and Atiya 1979; Gomez et al. 2006), pointing at the importance of lateral motion. It is believed to take up practically the entire lateral offset of the DST, because the difference between the stratigraphic sections across its southern extremity reveals a lateral offset similar to the offset farther south (Quennell 1959; Freund 1965; Freund et al. 1970; Walley 1983, 1988; Sneh and Weinberger 2003). GPS data (Reilinger et al. 2006; Gomez et al. 2007; Le Beon et al. 2008; Alchalbi et al. 2010) also show that it is the main site of lateral motion in Lebanon. Thus it is not possible to accept interpretations tending to minimize the role of lateral motion on the Yammouneh Fault (e.g. Dubertret 1970).

As the strike of the Yammouneh Fault – 30°–35°NE – deviates considerably clockwise from the ca. N-S strikes of the main DST faults to the south and north, it forms a prominent restraining bend (Quennell 1959; Freund et al. 1970). The resulting transpressive deformation extends to distances of 30–50 km on the two sides of the fault, and is combined with significant vertical motions. This produced the internally deformed, structurally and topographically high, Lebanon and Hemon-Anti Lebanon anticlinal ranges (up to ca. 3 km high) and the synclinal Bekaa Valley syncline between them (Fig. 5.5).

The Bekaa Valley syncline (Fig. 5.5) is a structural low whose axis forms a small angle with the Yammouneh fault. Many smaller scale NE-SW to NNE-SSW trending tight folds (some with overturned flanks), i.e. deviating clockwise from Yammouneh fault, are developed along its flanks (Dubertret 1955; Renouard 1955; Beydoun 1977). This structural pattern points at left-lateral shearing of the entire Bekaa syncline combined with some transverse shortening. The southern part of the syncline is crossed by a longitudinal fault (Hasbaya Fault) whose nature (strike-slip?) is not well constrained; it is sealed by 3.5–2.2 Ma old basalts. Small occurrences of basaltic volcanics occur also farther north along the Bekaa Valley syncline (Dubertret 1955), recording magma ascent close to the DST trace.

The Hermon-Anti Lebanon anticlinal ridge, ca. 30 km wide, comprises several secondary anticlines and is crossed by the Rachaya Fault and Serghaya Fault (Fig. 5.5). The Rachaya Fault branches off the eastern border fault of the Hula basin

and extends ca. 40 km through the western flank of the Hermon-Anti Lebanon anticlinal range. The presence of a small pull-apart along its southern part (Heimann et al. 1990) indicates left lateral slip, probably only a few km in view of the limited length of this fault. The Serghaya Fault, ca. 100 km long, extends northward from the SE side of the range across its anticlinal crest, but it becomes indistinct before reaching the Bekaa Valley syncline (Fig. 5.5). Gomez et al. (2001, 2006) identified up to 6 km of left lateral offsets of streams, which indicate continuing lateral motion. Walley (1998) suggested a total offset of ca. 25 km, which appears excessive in view of the limited northward extent of the fault, but this needs further study. In the south this fault extends to a strongly deformed area on the SE side of the Hermon-Anti Lebanon range where Kopp and Leonov (2000) reported thrusting of Jurassic beds over Neogene-Quaternary beds, though they gave no details. The relations of these structures with the Hula basin are hidden by the volcanics of the Golan Heights.

West of the Yammouneh Fault the 30–35 km wide Lebanon range comprises several folds and flexures, mostly sub-parallel to the range, and it is also considerably faulted (Fig. 5.5). The southern part of Lebanon is crossed obliquely by the ca. 35 km long Roum Fault which splays from the Yammouneh Fault and is still active (Nemer and Meghraoui 2006). It displaces left laterally river valleys, but the offset decreases northward (Garfunkel 1981) until there is no visible geologic discontinuity in the pre-DST rocks along its northward prolongation, though much fracturing is recorded (Dubertret 1955; Khair 2001; Griffiths et al. 2000). Thus it appears that the Roum Fault does not extend northward to the Mediterranean coast, so it could not have taken up much of the DST lateral motion (e.g. suggested by Butler et al. 1998). Rather, in view of the very different cross sections of the folds on its two sides it is interpreted as marking a discontinuity in the internal deformation of Lebanon. The area west and SW of the Roum Fault is the northern continuation of the Galilee. It is crossed by NE-SW faults that probably have a right lateral slip component, like the faults with this trend in the adjacent part of the Galilee.

The northern 2/3 of Lebanon forms a major anticlinal arch that is cut by a system of NNE-SSW trending oblique-right lateral faults, offsetting the axis of the arch and the monocline along its western side (Fig. 5.5). As each segment of the arch has a different cross section, it appears that the arch and the faults developed coevally. Some of these faults extend to the coast where they offset Neogene sediments, which shows that they acted coevally with the DST. Because of the lateral DST motion this area must have moved along the bend at the northern end of the Yammouneh fault, so its overall shape must have changed as the motion progressed and it must have been internally deformed, but the mechanism needs further study.

Paleomagnetic data show that the rocks building the Lebanon and Hermon-Anti Lebanon ranges rotated on vertical axes. In northern Lebanon Gregor et al. (1974) found rotations of ca. 60° and ca. 30° ccw (relative to the paleomagnetic poles of Africa) of Jurassic and Early Cretaceous rocks, respectively. Ron (1987) treated these data as a single population and inferred an average rotation of 53° ± 10° ccw, while in southern Mt. Hermon he found that Early Cretaceous rocks rotated 69° ± 13° ccw, and Baer et al. (1998) found rotations of ca. 60° ccw. In contrast, Henry et al. (2010) found an average ccw rotation of 28° ± 6.4° in all exposures of

Aptian and Albian rocks in the Lebanon and Hermon-Anti Lebanon ranges, and in many sites they also identified a Neogene re-magnetization indicating rotations of 11° ccw. Ron et al. (1984) found a ccw rotation of 22° ± 9° in the Galilee next to the border with Lebanon, which very likely applies also to the northward continuation of this domain into Lebanon (SW of the Roum fault). The age of these rotations is not constrained directly, but in analogy with the Galilee (Sect. 5.5.1.) they probably occurred mainly during the activity of the DST. However, Henry et al. (2010), following Gregor et al. (1974), advocated also a pre-Aptian rotation of ca. 30° ccw in northern Lebanon. Clearly, more paleomagnetic data and structural studies are needed.

5.5.2.2 The Syrian Segment

North of Lebanon the DST is also transpressional, but since it trends close to N-S the transverse shortening is much smaller (ca. 1/3) than in Lebanon segment. The two segments are separated by a structural low covered by the ca. 6–4 Ma old Homs (or Shin) basalts (Fig. 5.6, Mouty et al. 1992; Sharkov 2000). West of the DST the volcanics cover an erosion surface that cuts gradually down from Neogene sediments near the coast to Late Jurassic beds next to the DST fault, but ca. 2 km farther east the volcanics cover Middle Cretaceous beds, stratigraphically several hundred meters higher (Ponikarov 1964; Mouty et al. 1992; Chorowicz et al. 2005; Gomez et al. 2006). This shows that here an eroded structural step existed along the trace of the DST before basalt extrusion, indicating that here the DST was active already before the end of the Miocene. This, and the evidence regarding the lateral motion provided by the Miocene sections farther north (see 5.4) show that the Syrian segment of the DST was active considerably earlier than envisaged by Rukieh et al. (2005).

At the transition from Lebanon to the Syrian segment the principal DST fault changes strike quite abruptly, and a ca. 12 km long depression (pull-apart?) is developed (Fig. 5.6). Farther north the principal fault zone is 2–3 km wide and comprises several fractures. Ongoing activity is proven by the offset of a Roman aqueduct and of morphologic features, and also by minor structures (Trifonov et al. 1991; Meghraoui et al. 2003; Chorowicz et al. 2005; Rukieh et al. 2005), confirming that this is where the lateral DST motion now takes place. The shape of the Homs volcanic field strongly suggests that it was offset left laterally, estimated as >20 km by Chorowicz et al. (2005) but considerably less by Rukieh et al. (2005). An exact figure cannot be given because the edges of the volcanic field are much eroded.

Farther north the fault zone bifurcates into two major branches that enclose the ca. 50 km long and ca. 15 km wide Ghab basin pull-apart which has an up to 3.5 km thick young fill (Fig. 5.6, Dubertret 1955; Ponikarov 1964; Kopp and Leonov 2000; Brew et al. 2001a, b; Rukieh et al. 2005). Data from shallow wells show that the basin formed already in the early Pliocene, but the deeper part of its fill, still undated, may well be older. Structural interpretations vary. Brew et al. (2001a, b) inferred that the eastern boundary fault was sub-vertical and the western boundary

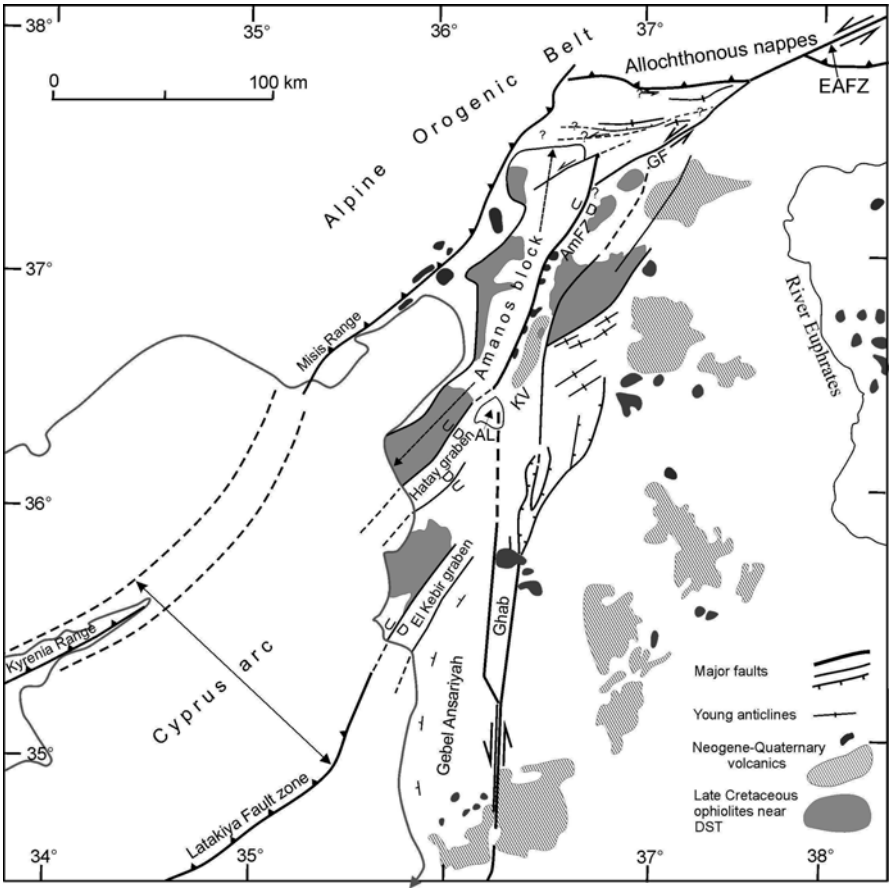

Fig. 5.6 Northern segments of the DST. *AL* Amik Lake, *AmFZ* Amanos fault zone, *EAFZ* East Anatolian fault zone, *GF* Gölbaşi fault, *KV* Karasu Valley

fault was normal, while Kopp and Leonov (2000) reported steep dips and mesoscale structures indicating reverse faulting along both boundary faults, and Zanchi et al. (2002) reported older thrusts and younger E-W extension. Clearly, further structural study is needed.

North of the Ghab basin the principal fault zone comprises a ca. 15 km wide belt of narrow N-S trending horsts and grabens formed by post-Miocene faulting (Fig. 5.6, Ponikarov 1964). Most of the faults in this zone are inactive, as at the northern end of the Ghab basin they are covered by 1–2 Ma old basalts that are not visibly faulted (Ponikarov 1964; Ponikarov et al. 1969; Sharkov 2000), while in the north they do not displace the fill of the Amik basin. East of this belt the possibly active Afrine Fault branches off the Ghab basin, (Fig. 5.6), but its role is insufficiently known. Only the westernmost fault, the prolongation of the western border fault of the Ghab basin, is active and extends northward to the Amik basin (Fig. 5.6, Senel 2002; Karabacak et al. 2010; see 5.5.2.3).

The transform eastern DST flank is little deformed, but its western flank – the uplifted Jebel Ansarieh (An-Nusseriyeh) range (coastal range of Syria) – is much faulted (Ponikarov 1964; Ponikarov et al. 1969). Kopp and Leonov (2000) concluded that the dominant NE-SW striking faults had a right-lateral slip component. They suggested that here blocks rotated ccw on vertical axes, like in N Lebanon, but this has not been investigated. In the north the Nahr al-Kabir (Latakie) graben (see Sect. 5.3) separates the Ansariyeh range from the Bassit block on which Late Cretaceous ophiolites are present (Fig. 5.1, Ponikarov 1964; Rukieh et al. 2005). The motion between these blocks is not known, but there is no obvious evidence that it was significant.

5.5.2.3 The Northern End of the DST

The northernmost, Turkish, segment of the DST is dominated by the Karasu graben, with the Amik basin in its southern part, which are flanked by the high standing Amanos Block in the west and the NE corner of the Arabian plate on the east (Fig. 5.6). These form the direct northward prolongation of the DST structure farther south. Left lateral motion continues northward from the Ghab basin into the Amik basin (Senel 2002; Karabacak et al. 2010), and farther north along the prominent NNE-SSW trending Amanus Fault Zone along the west side of the Karasu graben. Offset lava flows along this fault zone record left-lateral slip at a rate of ca. 2.9 mm/year in the last 1 Ma (Rojay et al. 2001; Seyrek et al. 2007, superseding previous studies). Lateral slip may also occur along the eastern side of the Karasu graben (Perinçek and Çemen 1990; Westaway and Arger 1996), but was not documented in detail. Tatar et al. (2004) inferred Quaternary shearing of the entire Karasu graben based on paleomagneric data, but this is very doubtful – the spread of the data is very large and supporting structural data are lacking.

The Amik basin (Fig. 5.6) is filled with 3–5 km of Neogene-Quaternary beds that overlie Late Cretaceous ophiolite nappes, but farther north the Karasu graben floor exposes the ophiolites and other pre-transform rocks (Coskun 1994; Perinçek and Çemen 1990; Rojay et al. 2001; Senel 2002). This requires a major structural step on the northern side of the Amik basin, but its history was not documented. Young volcanics, often of Quaternary age, extend along the Karasu graben, again demonstrating magma ascent along the DST. In the west the SW-NE trending Hatay graben (Asi graben) branches off the Amik basin (Fig. 5.6). It subsided and was crossed by NE-SW normal faults already in middle and late Miocene times, but the present graben structure was shaped in Pliocene-Quaternary times (Boulton et al. 2006).

The ca. NNE-SSW striking faults delimiting the Karasu graben, which appear to be the direct northward continuation of the DST structures, end abruptly in the north against an E-W trending anticline (near the town Kahraman Maras) (Fig. 5.6, Karig and Kozlu 1990; Yilmaz 1993; Senel 2002). Early plate tectonic models (Freund 1965; Wilson 1965; McKenzie et al. 1970) interpreted this area as a triple junction, called the Maras triple junction, between the Arabia and Sinai plates and the Alpine zone of plate convergence. However, the site of plate convergence – the front of the Alpine allochthonous nappes – is situated 20–25 km north of Maras (Fig. 5.6), and

the intervening area exposes Cenozoic sediments typical of the margin of the Arabian platform, which are deformed by N-S compression. Thus the situation is more complex than suggested in these models.

During the early stages of the DST activity, in the Miocene, continuing plate convergence along the Bitlis suture east of it led to emplacement of allochthonous nappes on the northern edge of the Arabian platform, while west of the DST plate convergence took place north of the Eastern Mediterranean basin (Şengör and Yilmaz 1981; Yilmaz 1993; Robertson 2001a, b; Robertson et al. 2004). In (late?) Early Miocene times, close to the time of the DST initiation, the Cyprus arc became the southern part of the orogenic belt and was thrust over the Levant basin (northern part of Sinai plate) along the Latakiya Fault zone (Fig. 5.6, Eaton and Robertson 1993; Robertson 2001b; Vidal et al. 2000; Hall et al. 2005a, b). Thus when the lateral DST motion began in the early Miocene, a triple junction as envisaged in the above models, probably existed along the belt of plate convergence.

However in the Pliocene, 3–4 Ma ago, the geometry of the plate boundaries near the northern end of the DST changed as westward extrusion of Anatolia became important and the left lateral East Anatolian Fault Zone, not yet recognized in the early works, Formed, but a slow change may have begun earlier. It cut obliquely the Alpine nappe front (i.e. the older) and continued into the NE corner of the Arabian platform, becoming the new Arabia-Anatolia plate boundary east of the DST (Fig. 5.6, Şengör et al. 1985; Bozkurt 2001; Hubert-Ferrari et al. 2009). This event was of great significance for the evolution of the entire East Mediterranean region (Le Pichon and Kreemer 2010), but is outside the scope of the present work, so only effects near the DST will be considered here. West of the DST plate convergence continued along the Cyprus arc, so the question arises as to how the new plate boundary east of it continues westward.

The lateral offset along the East Anatolian Fault Zone is estimated as 20–30 km (Şaroğlu et al. 1992; Westaway and Arger 1996). Offset alluvial fans some distance east of the DST, and GPS data record a young slip rate of 10–11 mm/year (Cetin et al. 2003; Reilinger et al. 2006; Reilinger and McClusky 2011; Le Pichon and Kreemer 2010), compatible with its young age. In the Early Pleistocene and earlier times the Kyrenia-Misis line and perhaps other structures took up some of the convergence (Fig. 5.6, Karig and Kozlu 1990; Hall et al. 2005a, b; Robertson 2001a, b; Robertson et al. 2004), but now the Anatolia-Levant basin convergence is concentrated on the Latakiya Fault Zone according to seismicity and GPS data (Papazachos and Papaioannou 1999; Reilinger et al. 2006). When the East Anatolian Fault Zone formed it must have linked with these structures and a component of lateral slip was most likely added to the motion along them, but how this happened is still not well understood.

Yilmaz (1993 his Fig. 2) and Senel (2002) show that ca. 100 km east of the Karasu graben the East Anatolian Fault Zone splits into several branches that extended north of its presently active trace – one that extends into the northern part of the Amanos Block and offsets its eastern boundary, and another one still farther north (Fig. 5.6). A fault may also extend close to the front of the Alpine nappes, where left lateral motion was reported, though its importance is debated (Karig and Kozlu 1990; Robertson et al. 2004). When these faults were active the motion along

the western part of the East Anatolian Fault Zone was partitioned between them, so the link with the structures west of the Amanos Block was apparently through a wide zone, in part extending north of the Amanos Block (Fig. 5.1), but the details still require clarification. As these faults have no clear morphologic expression they are probably inactive at present.

Now the Gölbaşi Fault (GF, Fig. 5.6), marked by a prominent physiographic feature, appears to be the active western strand of the East Anatolian Fault Zone (Perinçek and Çemen 1990; Şaroĝlu et al. 1992; Westaway and Arger 1996). It reaches the Amanus Fault Zone, but an active fault that forms its westward continuation into the Amanos Block was not clearly documented, and the two fault-controlled morphological margins of this block are not visibly offset. Thus it is not easy to accept that the Gölbaşi Fault continues westward across the Amanus Block (as suggested by Westaway 2003; Westaway et al. 2006), but this requires further study. Possibly, the motion along the Gölbaşi Fault is linked to the slip along Latakiye Fault Zone via the Amanus FZ and the Hatay graben (Perinçek and Çemen 1990; Şaroĝlu et al. 1992; Mahmoud et al. 2013).

The stress regime in the area provides additional insights and tends to support this picture. Field studies by Over et al. (2004) reveal that in Recent-Quaternary times a regime of left lateral transtension prevailed along the Hatay graben and the Amanus Fault Zone, compatible with GPS data (Reilinger and McClusky 2011; Mahmoud et al. 2013) and with the normal slip component on the Amanus Fault Zone inferred from field data by Perinçek and Çemen (1990), Rojay et al. (2001), Seyrek et al. (2007) (but not with thrusting on this fault, which Adiyaman and Chorowicz (2002) inferred from remote sensing data). However, if the Amanus Block were rigidly attached to the more southern part of the western DST flank, i.e. to the Sinai plate, then the plate kinematics require transpression in this area (Garfunkel 1981). Thus now this block appears to be decoupled from the Sinai plate and seems to move approximately like the Cyprus arc, which is supported by GPS data (Reilinger and McClusky 2011; Mahmoud et al. 2013). The decoupling probably drives the young activity of the Hatay graben, and possibly also the Nahr el-Kebir graben, though both are relatively old structures. However, this situation is probably young and has not yet produced significant motion relative to the western DST flank, as there is no identifiable geologic discontinuity along these structures. Indeed, the field data (Over et al. 2004) reveal a regime of transpression in Pliocene-Miocene times, indicating considerable coupling of the Amanos block with the western DST flank south of it. However, if the coupling was rigid most of this time, then 20 km or more of transverse shortening across the northernmost DST is expected. Seyrek et al. (2007) concluded that this was the case, but since their plate kinematic model conflicts with the GPS data (see above) and they did not present field data to constrain the amount of E-W shortening, this interpretation requires further study. Thus it seems that the Amanos block tended to behave independently for some time, and recently tends to become attached to the Cyprus arc. So a new Hatay triple junction seems to develop, though it utilizes older structures.

If a significant part of the lateral motion of the East Anatolian FZ was transferred westwards north of the Amanos Block, this would truncate the northern segment of

the DST and juxtapose it with a sliver of the Arabian platform that was originally located farther east. Before that the DST was closer to the area (ca. long 36.75°E) where the E-W trending nappes end more western structures farther west strike ca. NE-SW (Fig. 5.6, Yilmaz 1993; Karig and Kozlu 1990; Senel 2002; Robertson et al. 2004). This raises the possibility the shape of the nappe front was influenced to some extent by the DST and not only by the curved shape of the northern boundary of Arabia.

In summary, because of the young changes in the tectonic pattern, the young activity along the Turkish segment of the DST cannot be described in terms of the Sinai-Arabia plate boundary and a simple "Maras triple junction", but incomplete understanding of the new tectonic pattern in this area does not allow reliably restore the older situation. However, since this segment is the direct continuation of the DST structures farther south, and since it is the only major structure that could have accommodated the lateral offset across the north of the Syrian segment, it is believed that it should be considered as part of the DST during the early stages of its development. Additional data are required to resolve these issues.

5.5.2.4 Deformation Along the Northern Part of the DST

The foregoing account shows that deformation along the Lebanon and Syrian segments of the DST is complex, but is considered as a result of transpression because the DST trace deviates clock-wise from the local direction of the relative left lateral plate motion. However, this does not apply to the young history of the Turkish segment because of the young changes in this area (as explained in 5.5.2.3).

Given the orientation of the Yammuneh fault, plate kinematics requires that its flanks should be shortened by up to 40–50 km (Freund et al. 1970; Garfunkel 1981). The actual figure is probably less, because deformation of the adjacent Palmyrides, which began in the Cretaceous but continued during the time of DST activity (Chaimov et al. 1990; Searle 1994; Walley 1998; Kopp and Leonov 2000; Brew et al. 2001a; Rukieh et al. 2005) would bend the DST trace. However, even if a large part of the total ca. 20 km NW-SE shortening of the Palmyrides contributed to bending of this fault, this would amount to <10°, so the remaining transverse shortening of the fault flanks is still expected to be ca. 30 km or more.

The folding of the Yammouneh Fault flanks (Fig. 5.5) indeed records transverse shortening, but the fold geometry shows that it is doubtful that this could have exceeded 5 km. Thus the rest must be explained in another way. The most likely mechanism is rotation on vertical axes of small blocks between sub-parallel strike slip faults, as is revealed by paleomagnetic data. The large ccw rotations (Ron 1987; Henry et al. 2010) provide a very efficient mechanism of large-scale regional deformation (Ron et al. 1984; Garfunkel and Ron 1985). Such a deformation practically preserves surface area, so in contrast with folding and thrusting it does not lead to crustal thickening. Rotations of 25°–30° ccw, as Henry et al. (2010) found in Lebanon, would reduce the E-W dimension of the deformed zone while increasing its N-S length by tens of percent (Freund et al. 1970; Garfunkel and Ron 1985). So

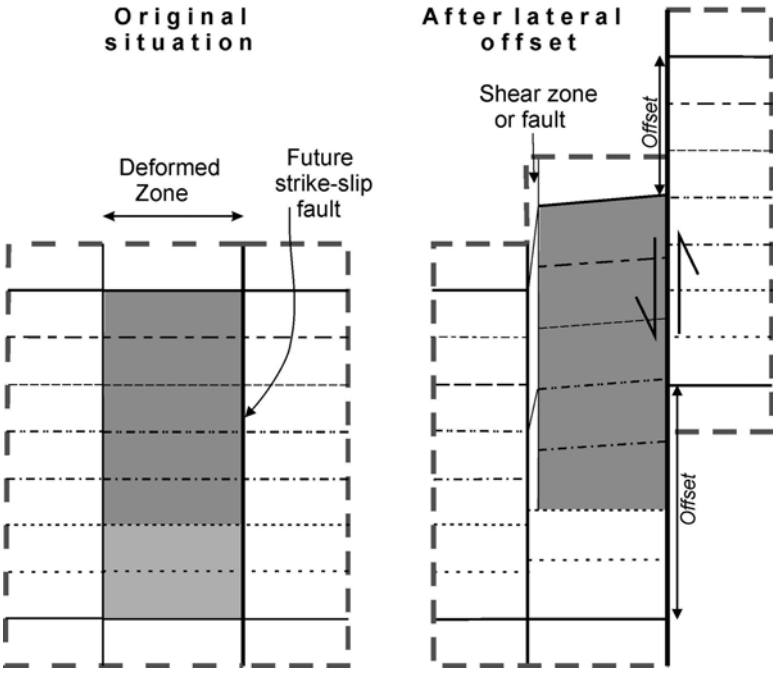

Fig. 5.7 Sketch to show how the amount of lateral offset of marker is affected by deformation of the margins of a strike-slip fault. The *light domain* is affected by fault-parallel extension, while the *darker gray domain* is also sheared. Along the main fault the offset varies, and a fault/shear zone develops along the margin of the deformed domain

qualitatively these results can explain the shortening perpendicular to the DST in Lebanon. The rotation assumed by Ron (1987), based on fewer data and combining measurement from different area, is more difficult to apply, so this matter needs clarification. Along the Syrian segment transpression was much smaller: some folding occurred NE of the Ghab depression, and considerable faulting affected its western flank, and here too rotation of blocks about vertical axes was suggested, but there are no data directly supporting this assumption.

If the left lateral shearing by block rotations indeed results in N-S lengthening of its western flank, then left-lateral shearing must arise along its junction with the adjacent undeformed Levant basin north of the Galilee, as is seen on Fig. 5.7. In this case the lateral offset on the main fault is reduced (see 5.5.1.6) while the total left lateral offset parallel to the DST appears to be preserved (Fig. 5.7). Deformation of the continental margin was indeed observed and was interpreted as related to the deformation onland (Schattner et al. 2006; Carton et al. 2009; Elias et al. 2007), but its magnitude needs further testing.

The considerable deformation of the flanks of the Lebanon and Syrian segments, affecting an up to 65–75 km wide zone at shallow levels, is expected to affect also deeper crustal levels. The occurrence of volcanics close to and along the main trace of the DST from the central Jordan Valley and northward, which shows that the DST

was a preferred pathway for magma ascent, raises the possibility that igneous intrusions and resulting heating could have influenced the mechanical properties of the crust under the DST flanks. However, these issues cannot be further explored in the absence of relevant data.

5.6 Discussion

The foregoing summary, though often limited because of insufficient data, highlights some basic questions regarding the plate setting, history, and development of the entire DST, and also stresses major challenges facing future research.

As noted, the DST was superimposed on, and cuts through, older structures. There is no known evidence that any part of it reactivated older structures, though such structures could have influenced the shape of its trace and the details of deformation along it. The bend along the Yammouneh Fault formed where the DST crosses a Permian-Triassic rift underlying the Palmyrides, so it is likely that it was influenced by the older rift. The known data do not resolve differences in the times of initiation of the various parts of the DST before they joined to form a throughgoing plate boundary. However, if such early lateral offsets were significant (more than a few kilometers) along distinct segments, then next to their terminations visible structures should have formed to accommodate the lateral motions. The only known structures that could have formed (or were accentuated) in this way are the Palmyrides, which could have allowed some early slip on the southern part of the DST. However, since the Palmyrides were deformed also during the DST activity, this could have amounted to only a fraction of the entire ca. 20 km of NW-SE shortening east of the DST trace, which is a small fraction of the total offset. This could delay the northward propagation of the DST by a few Ma only, which is compatible with the lines of evidence mentioned above, that point at its Miocene activity (including its northern pars: see 5.3, 5.5.2.2, and 5.5.2.3). Therefore it is impossible to accept models proposing that the northern part of the DST did not form before the Late Miocene, i.e. when a large lateral offset had already taken place along its southern part (e.g. Kopp and Leonov 2000; Homberg et al. 2010).

It is concluded, therefore, that the entire DST formed over a short, though unknown, period, most likely late in the Early Miocene (17–18 Ma ago). Since then the DST acted as a continuous transform boundary between the Sinai and Arabia plates, except for its Turkish segment (see below). Thus the Sinai-Arabia plate kinematics provides a framework for its interpretation. Since this boundary has an irregular shape in map view, its two sides cannot fit when lateral motion progresses. The result will be either transtension or transpression, depending on the relation between the direction of the relative plate motion and the local trend of the plate boundary. This will lead to different types of deformation along the DST and its flanks that varies along its trace. The foregoing review showed that the kinematics of the Sinai-Arabia plate motion, as constrained by combining data from the DST itself with data from the Red Sea, indeed provide a framework for relating the major structures along the DST to the irregularities of its trace.

In particular, the formation and growth of a string of deep depressions along the southern part of the DST expresses its predominantly transtensional character that is predicted by the plate kinematics. These basins accommodate most of the oblique separation of its flanks which increases as the lateral motion along the DST progresses. In contrast, along the northern part of the DST, where plate kinematics predicts transpression, the deformation is very different and extends some distance into the DST flanks. The expected shortening normal to the DST trace is accommodated by folds with axes sub-parallel to the main DST fault and especially by rotation of fault blocks on vertical axes, which is proven by paleomagnetic data. It turns out that the latter type of deformation leads to a result not appreciated before: it can increase the N-S length of the western DST flank, which in turn will produce left lateral shearing along the junction with the undeformed Levant basin (see 5.5.2.4 and Fig. 5.7). This comes at the expense of the lateral motion along the main DST faults, which may well explain the decrease of the lateral offset observed along the northern part of DST (see 5.3).

Thus, qualitatively the observed structures can produce the effects expected from plate kinematic considerations, but like in many places in the world is difficult to constrain. Therefore it cannot be ascertained that the observed structures indeed agree quantitatively with the plate kinematic predictions, especially regarding the northern part of the DST (e.g. the ca. 30–40 km shortening perpendicular to the DST across the Lebanon segment or the apparent northward decrease of the lateral offset). This difficulty led to many discussions, but it cannot be taken as an argument against the occurrence of large lateral motion along the northern part of the DST (as suggested e.g. by Dubertret 1970). Rather it reflects incomplete quantitative understanding of the te observed structures – a frequently encountered difficulty. This remains a major challenge for future research.

The northernmost (Turkish) segment of the DST requires separate treatment. Since the structures of the Turkish segment are the direct continuation of the DST farther south, and they are the only known structures that could have taken up the lateral DST offset documented just south of them, they are considered to have been in integral part of the DST during its early history. However, ca. 4 Ma ago the plate configuration and motions in that region changed when the westward extrusion of Anatolia became important and the East Anatolian FZ formed. This affected the northernmost portion of the DST, so now it is no longer a part the Sinai-Arabia plate boundary. Though the young kinematics in this area is insufficiently known, it appears that the Amanos Block – its western flank – was decoupled from the Sinai plate and tended to join the Anatolian plate (i.e. the Cyprus arc). Originally this block was probably attached, though perhaps not rigidly, to the western DST flank, given the Miocene age of the Hatay graben and the Nahr el-Kebir graben south of it. The young tectonic changes obscured the structural relations in this region during the early stages of the DST history, including its interaction with the Alpine orogenic belt. Much more data are required to resolve these issues.

In summary, the Sinai-Arabia plate kinematics provides a useful framework for analyzing the history and deformation along the DST and its flanks, though many issues need further study. However, full understanding of the structure – e.g. the fault arrangement, the partitioning of deformation between different structures, the width of the deformed zones, and changes in the structure with time – requires

dynamic modeling that takes into consideration the mechanical properties of the crust (and the entire lithosphere), the regional stress field, igneous activity, and other processes in the underlying mantle.

Acknowledgements I am very grateful to X. Le Pichon and A. Sagy for their helpful reviews.

References

Adiyaman Ö, Chorowicz J (2002) Late Cenozoic tectonics and volcanism in the northwestern corner of the Arabian plate: a consequence of the strike-slip Dead Sea fault zone and the lateral escape of Anatolia. J Volcanol Geotherm Res 117:327–345

Al Tarazi E, Abu Rajab J, Gomez F, Cochran W, Jaafar R, Ferry M (2011) GPS measurements of near-field deformation along the southern Dead Sea fault system. Geochem Geophys Geosyst 12:Q12021. doi:10.1029/2011GC003736

Alchalbi A, 15 others (2010) Crustal deformation in northwestern Arabia from GPS measurements in Syria: slow slip rate along the northern Dead Sea fault. Geophys J Int 180:125–135. doi:10.1111/j.1365-246X.2009.04431.x

Aldersons F, Ben-Avraham Z, Hofstetter A, Kissling E, Al-Jazreen A (2003) Lower-crustal strength under the Dead Sea basin from local earthquake data and rheological modeling. Earth Planet Sci Lett 214:129–142. doi:10.1016/S0012-821X(03)00381-9

Al-Maleh K, Delaune M, Mouty M, Parrot JF (1992) Relations du front de la nappe ophiolitique du nord-ouest syrien avec son substratum de la part et d'autre de la faille du levant: Baer-Bassit, Kurd-Dagh. Compt Rendus Acad Sci Paris 314:1195–1202

Al-Zoubi A, ten-Brink US (2002) Lower crustal flow and the role of shear in basin subsidence: an example from the Dead Sea Basin. Earth Planet Sci Lett 199:67–79

Al-Zoubi A, Heinrich T, Qabbami I, Ten-Brink US (2007) The northern end of the Dead Sea basin: geometry from reflection seismic evidence. Tectonophysics 434:55–69

ArRajehi A, 16 others (2010) Geodetic constraints on present-day motion of the Arabian plate: implications for Red Sea and Gulf of Aden rifting. Tectonics 29:TC3011. doi:10.1029/2009TC002482

Avni Y, Garfunkel Z, Bartov Y, Ginat H (1994) Pleistocene fault system in the central and southern Negev and its implications for the tectonic and geomorphic history of the Arava rift margin. Geol Surv Isr Curr Res 9:51–58

Avni Y, Bartov Y, Garfunkel Z, Ginat H (2000) The Arava Formation – A Pliocene sequence in the Arava Valley and its western margin, southern Israel. Isr J Earth Sci 50:101–120

Avni Y, Segev A, Ginat H (2012) Oligocene regional denudation of the northern Afar dome: pre- and syn- breakup stages of the Afro-Arabian plate. Geol Soc Am Bull 124:1871–1897

Baer G, Hirsch F, Ron H (1998) The Newe Ativ graben, Mt. Hermon: its origin and implications for the regional structure. Isr J Earth Sci 46:61–78

Bandel K (1981) New stratigraphic and structural evidence for lateral dislocation in the Jordan rift connected with description of the Jurassic rock column in Jordan. N Jb Geol Paläont (Abh) 161:271–308

Bandel K, Khouri H (1981) Lithostratigraphy of the Triassic in Jordan. Facies 4:1–26

Bartov Y (1974) A structural and paleogeographic study of the central Sinai faults and domes. Dissertation, Hebrew Univ Jerusalem (in Hebrew, Eng abs), 143 p

Bartov Y (1994) The geology of the Arava. Geol Sur Isr report GSI/4/94, 16 p. (in Hebrew)

Bartov Y, Sagy A (2004) Late Pleistocene extension and strike-slip in the Dead Sea basin. Geol Mag 141:565–572

Bartov Y, Avni Y, Calvo R, Frieslander U (1998) The Zofar Fault – A major intra-rift feature in the Arava rift valley. Geol Surv Isr Curr Res 11:27–32

Basha S (1982) Stratigraphy, paleogeography and oil possibilities of the Azraq-sirhan-Turayf basin (Jordan-Saudi Arabia). Dirasat 9:85–106

Bein A, Gvirtzman G (1977) A Mesozoic fossil edge of the Arabian plate along the Levant coast and its bearing on the evolution of the Eastern Mediterranean. In: Biju-duval B, Montadert L (eds) Symposium on the history of the Mediterranean basins. Split. Edit Technip, Paris, pp 95–109

Belitzky S (1987) Tectonics of the Korazim saddle. Dissertation, Hebrew Univ Jerusalem 94 p (in Hebrew)

Ben-Avraham Z (1985) Structural framework of the Gulf of Elat (Aqaba), northern Red Sea. J Geophys Res 90:703–726

Ben-Avraham Z, Almagor G, Garfunkel Z (1979) Sediments and structure of the Gulf of Elat. Sediment Geol 23:239–267

Ben-Avraham Z, Garfunkel Z (1986) Character of transverse faults in the Elat pull-apart basin. Tectonics 5:1161–1169

Ben-Avraham Z, Hanel R, Vilinger H (1978) Heat flow through the Dead Sea rift. Mar Geol 28:253–269

Ben-Avraham Z, Ten Brink U, Bell R, Reznikov M (1996) Gravity field over the Sea of Galilee: evidence for a composite basin along a transform fault. J Geophys Res 101:533–544

Ben-Avraham Z, Garfunkel Z, Lazar M (2008) Geology and evolution of the southern Dead Sea fault with emphasis on subsurface structure. Ann Rev Earth Planet Sci 36:357–387

Ben-Avraham Z, Lazar M, Garfunkel Z, Reshef M, Ginzburg A, Rotstein Y, Frieslander U, Bartov Y, Shulman H (2012) Chapter 17: Structural styles along the Dead Sea fault. In: Roberts DG, Bally AW (eds) Regional geology and tectonics: phanerozoic passive margins, cratonic basins and global tectonic maps, vol 1C. Elsevier, Burlington, pp 617–634

Bender F (1974) Geology of Jordan. Gebrüder Borntraeger, Berlin/Stuttgart, 196 p

Bentor YK (1985) The crustal evolution of the Arabo-Nubian massif with special reference to the Sinai Peninsula. Precambian Res 28:1–74

Beydoun ZR (1977) Petroleum prospects of Lebanon: reevaluation. Am Assoc Petrol Geol Bull 61:43–64

Bosworth W (2005) The Red Sea and Gulf of Aden. J Afr Earth Sci 43:334–378

Boulton SJ, Robertson AHF, Ünlügenç U (2006) Tectonic and sedimentary evolution of the Cenozoic Hatay Graben, southern Turkey: a two phase model for graben formation. Geol Soc Lond Spec Publ 260:613–634

Bozkurt E (2001) Neotectonics of Turkey – a synthesis. Geodinamica Acta 14:3–30. doi:10.1016/S0985-3111(01)01066-X

Brew G, Barazangi M, Al-Maleh K, Sawaf T (2001a) Tectonic and geologic evolution of Syria. GeoArabia 6:573–616

Brew G, Lupa J, Barazangi M, Sawaf T, Al-Imam A, Zaza T (2001b) Structure and tectonic development of the Ghab basin and the Dead Sea fault system, Syria. J Geol Soc 158:665–674

Butler RWH, Spencer S, Griffiths HM (1998) The structural response to evolving plate kinematics during transpression: evolution of the Lebanese restraining bend of the Dead Sea transform. Geol Soc Lond Spec Publ 135:81–106

Calvo R (2002) Stratigraphy and petrology of the Hazeva formation in the Arava and the Negev. Geol Surv Isr report GSI/22/02, 264 p (in Hebrew, Engl abst)

Carton H, Singh SC, Tapponnier P, Elias A, Briais A, Sursock A, Jomaa R, King GCP, Daeron M, Jacques E, Barrier E (2009) Seismic evidence for Neogene and active shortening offshore of Lebanon (Shalimar cruise). J Geophys Res 114:B07407. doi:10.1029/2007JB005391

Cetin H, Guneyli H, Mayer L (2003) Paleoseismology of the Palu-Lake Hazar segment of the East Anatolian fault zone, Turkey. Tectonophysics 374:163–197

Chaimov TA, Barazangi M, Al-Saad D, Sawaf T, Gebran A (1990) Balanced cross sections and shortening in the Palmyride fold belt of Syria and implications for movement along the Dead Sea fault system. Tectonics 9:1369–1386

Chorowicz J, Dhont D, Ammar O, Rukieh M, Bilal A (2005) Tectonics of the Pliocene Homs basalts (Syria) and implications fro the Dead Sea fault zone activity. J Geol Soc 162:259–271

Chu D, Gordon RG (1998) Current plate motions across the Red Sea. Geophys J Int 135:313–328

Cochran JR (1983) A model for the development of the Red Sea. Am Assoc Petrol Geol Bull 67:41–49

Cochran JR (2005) Northern Red Sea: nucleation of an oceanic spreading center within a continental rift. Geochem Geophys Geosys 6(3). doi:10.1029/2004GC000826
Cole GA, Abu-Al MA, Colling EL, Halpern HI, Carrigan WJ, Savage GR, Scolaro RJ, Al-Sharidi SH (1995) Petroleum geochemistry of the Midyan and Jaizan basins of the Red Sea, Saudi Arabia. Mar Pet Geol 12:597–614
Coskun B (1994) Oil possibilities of duplex structures in the Amik-Reyhanli basin, SE Turkey. J Pet Geol 17:461–472
Crowell JC (1974) Origin of late Cenozoic basins in southern California. Soc Econ Paleont Mineralog, Spec Publ 22:190–204
Druckman Y (1974) The stratigraphy of the Triassic sequence in southern Israel. Isr Geol Surv Bull 64:1–92
Dubertret L (1932) Les formes structurales de la Syria et de la Palestine: leur origine. Compt Rendus Acad Sci Paris 195:65–67
Dubertret L (1955) Carte géologique du Liban, scale 1:200 000, with explanatory notes. Ministry of Public Works, Beirut
Dubertret L (1970) Review of structural geology of the Red Sea and surrounding areas. Phil Trans R Soc London A267:9–20
Dullo WC, Hötzl H, Jado AR (1983) New stratigraphical results from the Tertiary sequence of Midyan area, NW Saudi Arabia. Newslett Stratigr 12:83
Eaton S, Robertson AHF (1993) The Miocene Pakhna Formation, southern Cyprus, and its relationship to the Neogene tectonic evolution of the Eastern Mediterranean. Sediment Geol 86:273–296
Eckstein Y (1979) Review of the heat flow data from the Eastern Mediterranean region. Pure Appl Geophys 117:150–179
Ehrhardt A, Hubscher C, Ben-Avraham Z, Gajewski D (2005) Seismic study of pull-apart-induced sedimentation and deformation in the Northern Gulf of Aqaba (Elat). Tectonophysics 396:59–79
Elias A, Tapponnier P, Singh SC, King GCP, Briais A, Daëron M, Carton H, Sursock A, Jacques E, Jomaa R, Klinger Y (2007) Active thrusting offshore Mount Lebanon: source of the tsunamigenic A.D. 551 Beirut-Tripoli earthquake. Geology 35:755–758. doi:10.1130/G23631A.1
Ellenblum R, Marco S, Agnon A, Rockwell T, Boas A (1998) Crusader castle torn apart by earthquake at dawn, 20 May 1202. Geology 26:303–306
Eyal M, Eyal Y, Bartov Y, Steinitz G (1981) The tectonic development of the western margin of the Gulf of Elat (Aqaba) rift. Tectonophysics 80:39–66
Fleischer E (1968) The subsurface geology of the HulA Valley and the Korazijm area. Geol Surv Isr report 15 p (in Hebrew)
Förster A, Forster HJ, Massarwe R, Masri A, Tarawneh K (2007) The surface heat flow of the Arabian shield in Jordan. J Asian Earth Sci 30:271–284
Freund R (1965) A model for the development of Israel and adjacent areas since the Upper Cretaceous times. Geol Mag 102:189–205
Freund R (1970) Plate tectonics of the Red Sea and East Africa. Nature 228:453
Freund R, Garfunkel Z, Zak I, Goldberg M, Weissbrod T, Derin B (1970) The shear along the Dead Sea rift. Phil Trans R Soc London A267:107–130
Frieslander U (2000) The structure of the Dead Sea transform emphasizing the Arava. Dissertation, Hebrew Univ Jerusalem, 106 p (in Hebrew English abstract)
Frieslander U, Ben-Avraham Z (1989) Magnetic field over the Dead Sea and vicinity. Mar Pet Geol 6:148–160
Fuis GS, Mooney WD, Heaky JH, McMechan GA, Lutter WJ (1984) A seismic refraction survey of the Imperial Valley region, California. J Geophys Res 89:1165–1189
Galli P (1999) Active tectonics along the Wadi Araba-Jordan valley transform fault. J Geophys Res 104:2777–2796
Gardosh M, Reches Z, Garfunkel Z (1990) Holocene tectonic deformation along the western margins of the Dead Sea. Tectonophysics 180:123–137
Gardosh M, Kashai E, Salhov S, Shulamn H, Tennenbaum E (1997) Hydrocarbon exploration in the southern Dead Sea area. In: Niemi T, Ben-Avraham Z, Gat JR (eds) The Dead Sea. Oxford University Press, New York, pp 57–72

Gardosh MA, Garfunkel Z, Druckman Y, Buchbinder B (2010) Neotethyan rifting and its role in shaping the Levant Basin and margin. Geol Soc Lond Spec Publ 341:9–36. doi:10.1144/SP341.2

Garfunkel Z (1981) Internal structure of the Dead Sea leaky transform (rift) in relation to plate kinematics. Tectonophysics 80:81–108

Garfunkel Z (1987) Post-Precambrian sediments. In: Bentor YK, Eyal M (eds) Jebel Sabbagh sheet, explanatory note. Israel Academy of Sciences and Humanities, Jerusalem, pp 386–392

Garfunkel Z (1988) The pre-Quaternary geology of Israel. In: Yom-Tov Y, Tchernov E (eds) The zoogeography of Israel. W Junk, Dordrecht/Holland, pp 7–34

Garfunkel Z (1989) Tectonic setting of Phanerozoic magmatism in Israel. Isr J Earth Sci 38:51–74

Garfunkel Z (1998) Constraints on the origin and history of the Eastern Mediterranean basin. Tectonophysics 298:5–36

Garfunkel Z (1999) History and paleogeography during the Pan-African orogen to stable platform transition: reappraisal of the evidence from the Elat area and the northern Arabo-Nubian Shield. Isr J Earth Sci 48:135–157

Garfunkel Z (2011) The long- and short-term lateral slip and seismicity along the Dead Sea transform: an interim reevaluation. Isr J Earth Sci 58:217–235. doi:10.1560/IJES.58.3-4.217

Garfunkel Z, Bartov Y (1977) The tectonics of the Suez rift. Isr Geol Surv Bull 71:1–44

Garfunkel Z, Ben-Avraham Z (1996) The structure of the Dead Sea basin. Tectonophysics 266:155–176

Garfunkel Z, Ban-Avraham Z (2001) Basins along the Dead Sea Transform. In: Ziegler PA, Cavazza W, Robertson AHF, Crasquin-Soleau S (eds) Peri-Tethys Memoir 6: Peri Tethyan rift/wrench basins and passive margins, Mémoires du Muséum national d'histoire naturelle 186. Publications scientifiques du Muséum, Paris, pp 607–627

Garfunkel Z, Beyth M (2006) Constraints on the structural development of Afar imposed by the kinematic of the major surrounding plates. In: Yirgu G, Ebinger CJ, Maguire PKH (eds) The Afar volcanic province within the East African System, Geological Society special publication 259. Geological Society, London, pp 23–42

Garfunkel Z, Derin B (1984) Permian-Early Mesozoic tectonism and continental margin formation in Israel and its implications for the history of the eastern Mediterranean. Geol Soc Lond Spec Publ 17:187–201

Garfunkel Z, Ron H (1985) Block rotation and deformation by strike slip fault 2. The properties of a type of macroscopic discontinuous deformation. J Geophys Res 90:8589–8602

Garfunkel Z, Zak I, Freund R (1981) Active faulting in the Dead Sea rift. Tectonophysics 80:1–26

Gaulier JM, LePichon X, Lyberis N, Averdik F, Geli L, Moretti I, Deschamps A, Hafez S (1988) Seismic study of the crustal thickness, Northern Red Sea and Gulf of Suez. Tectonophysics 153:55–88

Ginat H, Avni Y (1994) The Arava conglomerate: a Pliocene valley deposit crossing the Dead Sea rift. Geol Surv Isr Curr Res 9:59–62

Ginzburg A, Ben-Avraham Z (1997) A seismic refraction study of the north basin of the of the Dead Sea, Israel. Geophys Res Lett 24:2063–2066

Ginzburg A, Reshef M, Ben-Avraham Z, Schattner U (2006) The style of transverse faulting in the Dead Sea basin from seismic reflection data: the Amatzyahu fault. Isr J Earth Sci 55:129–139

Glickson YA (1966) The lacustrine Neogene of Kefar Giladi area. Isr J Earth Sci 15:135–154

Goldberg M, Beyth M (1991) Tiran Island: an internal block at the junction of the Red Sea rift and Dead Sea transform. Tectonophysics 198:261–273

Gomez F, Meghraoui M, Darkal AN, Tabet C, Khawlie M, Khair K, Sbeinati R, Darawcheh R, Khair K, Barazangi M (2001) Coseismic displacements along the Serghaya fault: an active branch of the Dead Sea fault system in Syria and Lebanon. J Geol Soc Lond 158:405–408

Gomez F, Khawlie M, Tabet C, Darkal AN, Khair K, Barazangi M (2006) Late Cenozoic uplift along the northern Dead Sea transform in Lebanon and Syria. Earth Planet Sci Lett 241:913–931

Gomez F, Karam G, Khawlie M, McClusky S, Vernant P, Reilinger R, Jaafar R, Tabet C, Khair K, Barazangi M (2007) Global Positioning System measurements of strain accumulation and slip

transfer through the restraining bend along the Dead Sea fault system in Lebanon. Geophys J Int 168:1021–1028. doi:10.1111/j.1365-246X.2006.03328.x

Gregor CB, Mertzman S, Nairn AEM, Negendank J (1974) Paleomagnetism and the Alpine tectonics of Eurasia. V. The paleomagnetism of some Mesozoic and Cenozoic volcanic rocks from the Lebanon. Tectonophysics 21:375–396

Gregory JW (1921) The rift Valleys and geology of East Africa. Seeley, London, 479 p

Griffiths HM, Clark RA, Thorp MK, Spencer S (2000) Strain accommodation at the lateral margin of an active transpressive zone: geological and seismological evidence from the Lebanese restraining bend. J Geol Soc Lond 157:289–302

Guiraud R, Issawi B, Boswoth W (2001) Phanerozoic history of Egypt and surrounding areas. In: Ziegler PA, Cavazza W, Robertson AHF, Crasquin-Soleau S (eds) Peri-Tethys Memoir 6: Peri Tethyan rift/wrench basins and passive margins, Mémoires du Muséum national d'histoire naturelle 186. Publications scientifiques du Muséum, Paris, pp 469–509

Hall J, Aksu AE, Calon TJ, Yasar D (2005a) Varying tectonic control on basin development at an active microplate margin: Latakia Basin, Eastern Mediterranean. Mar Geol 221:15–60

Hall J, Calon TJ, Aksu AE, Meade SR (2005b) Structural evolution of the Latakia Ridge and Cyprus Basin at the front of the Cyprus Arc, Eastern Mediterranean Sea. Mar Geol 221:261–297

Hancock PL, Atiya MS (1979) Tectonic significance of mesofracture systems associated with the Lebanese segment of the Dead Sea transform faults. J Struct Geol 1:143–153

Harash A, Bar Y (1988) Faults, landslides and seismic hazards along the Jordan River gorge, northern Israel. Eng Geol 25:1–15

Hardenberg MF, Robertson AHF (2007) Sedimentology of the NW margin of the Arabian plate and the SW-NE trending Nahr El-Kebir half-graben in northern Syria during the latest Cretaceous and Cenozoic. Sediment Geol 201:231–266

Harding TP, Vierbuchen RC, Christie-Blick N (1985) Structural styles, plate tectonic settings and hydrocarbon traps of divergent (transtensional) wrench faults. Soc Econ Paleontol Mineral 37:51–77

Hatcher RD, Zeiz I, Reagan RD, Abu-Ajameh M (1981) Sinistral strike-slip motion on the Dead Sea rift: confirmation from new magnetic data. Geology 9:458–462

Heimann A, Braun D (2000) Quaternary stratigraphy of the Kinnarot Basin, Dead Sea transform, northeastern Israel. Isr J Earth Sci 49:31–44

Heimann A, Ron H (1993) Geometrical changes of plate boundaries along part of the northern Dead Sea transform: geochronological and paleomagnetic evidence. Tectonics 12:477–491. doi:10.1029/92TC01789

Heimann A, Steinitz G (1989) $^{40}Ar/^{39}Ar$ total gas ages of basalts from Notera #3 well, Hula Valley, Dead Sea Rift: stratigraphic and tectonic implications. Isr J Earth-Sci 38:173–184

Heimann A, Eyal M, Eyal Y (1990) The evolution of Barahta rhomb-shaped graben, Mount Hermon, Dead Sea Transform. Tectonophysics 141:101–110

Heimann A, Steinitz G, Mor D, Shaliv G (1996) The Cover Basalt Formation, its age and its regional and tectonic setting: implications from K-Ar and $^{40}Ar/^{39}Ar$ geochronology. Isr J Earth Sci 45:55–71

Heimann A, Zilberman E, Amit R, Frieslander U (2009) Northward migration of the southern diagonal fault of the Hula pull-apart basin, Dead Sea Transform, northern Israel. Tectonophysics 476:496–511

Hempton MR (1987) Constraints on Arabian plate motion and extensional history of the Red Sea. Tectonics 6:687–705

Henry B, Homberg C, Mroueh M, Hamdan W, Higazi F (2010) Rotations in Lebanon inferred from new palaeomagnetic data and implications for the evolution of the Dead Sea Transform system. Geol Soc Lond Spec Publ 341:269–285

Heybroek F (1942) La Geologie d'une partie du Liban sud. Leidsche Geol Medded 12:251–470

Hofstetter R, Klinger Y, Amrat AQ, Rivera L, Dorbath L (2007) Stress tensor and focal mechanisms along the Dead Sea fault and related structural elements based on seismological data. Tectonophysics 429:165–181

Hofstetter R, Gitterman Y, Pinsky V, Kraeva N, Feldman L (2008) Seismological observations of the northern Dead Sea basin earthquake on 11 February 2004 and its associated activity. Isr J Earth Sci 57:101–124. doi:10.1560/IJES.57.2.101

Homberg C, Barrier E, Mroueh M, Muller C, Hamdan W, Higazi F (2010) Tectonic evolution of the central Levant domain (Lebanon) since Mesozoic time. Geol Soc Lond Spec Publ 341:245–268

Horowitz A (1973) Development of the Hula basin. Isr J Earth Sci 22:107–139

Horowitz A (1987) Palynological evidence for the age and rate of sedimentation along the Dead Sea rift, and structural implications. Tectonophysics 141:107–115

Horowitz A, Horowitz M (1985) Subsurface late Cenozoic palynostratigraphy of the Hula Basin. Pollen Spores 27:365–390

Hubert-Ferrari A, King G, Van DerWoerd J, Villa I, Altunel E, Armijo R (2009) Long-term evolution of the North Anatolian Fault: new constraints from its Eastern termination. Geol Soc Lond Spec Publ 311:133–154

Hughes GW, Perincek D, Grainger DJ, Abu-Bshait AJ, Jared ARM (1999) Lithostratigraphy and depositional history of part of the Midyan region, northwestern Saudi Arabia. GeoArabia 4:503–542

Hurwitz S, Garfunkel Z, Ben-Gai Y, Reznikov M, Rotstein Y, Gvirtzman H (2002) The tectonic framework of a complex pull-apart basin: seismic reflection observations in the northern Kinarot-Beit-Shean Basin, Dead Sea Transform. Tectonophysics 359:289–306

Jennings CW, compiler (1973) State of California, fault and geologic map, scale 1:750 000. California Division of Mines Geology, Sacramento

Joffe S, Garfunkel Z (1987) The plate kinematics of the circum Red Sea – A reevaluation. Tectonophysics 141:5–22

Karabacak V, Altunel E, Meghraoui M, Akyüz HS (2010) Field evidences from northern Dead Sea Fault Zone (South Turkey): new findings for the initiation age and slip rates. Tectonophysics 480:172–182

Karig DE, Kozlu H (1990) Late-Palaeogene-Neogene evolution of the triple junction region near Maras, south-central turkey. J Geol Soc Lond 147:1023–1034

Kashai EL, Crocker PF (1987) Structural geometry and evolution of the Dead Sea-Jordan rift system as deduced from new subsurface data. Tectonophysics 141:33–60

Khair K (2001) Geomorphology and seismicity of the Roum fault as one of the active branches of the Dead Sea fault system in Lebanon. J Geophys Res 106:4233–4245

Kopp ML, Leonov YG (2000) Tectonics. In: Leonov YG (ed) Outline of geology of Syria, Russ Acad Sci Geol Inst Trans 526, pp 7–104, Nauka, Moscow (in Russian)

Krasheninnikov VA (2005) F: Neogeve. In: Krasheninnikov VA, Hall JK, Hirshc F, Benjamini H, Flexer A (eds) Geological framework of the Levant, V.1 Cyprus and Syria. Historic al Productioin-Hall, Jerusalem, pp 343–392

Larsen BD, Ben-Avraham Z, Shulman H (2002) Fault and salt tectonics in the southern Dead Sea basin. Tectonophysics 346:71–90

Lazar M, Ben-Avraham Z, Schattner U (2006) Formation of sequential basins along a strike-slip fault – Geophysical observations from the Dead Sea basin. Tectonophysics 421:53–69

Le Beon M, Klinger Y, Amrat AQ, Agnon A, Dorbath L, Baer G, Ruegg JC, Charade O, Mayyas O (2008) Slip rate and locking depth from GPS profiles across the southern Dead Sea Transform. J Geophys Res 113:B11403. doi:10.1029/2007JB005280

Le Pichon X, Kreemer C (2010) The Miocene to present kinematic evolution of the eastern Mediterranean and Middle East and its implication for dynamics. Ann Rev Earth Planet Sci 38:323–351

Le Pichon X, Gaulier JM (1988) The rotation of Arabia and the Levant fault system. Tectonophysics 153:271–294

Le Pichon X, Bergerat F, Roulet MJ (1988) Plate kinematics and tectonics leading to the Alpine belt formation. A new analysis. Geol Soc Am Spec Pap 218:111–131

Le Pichon X, Francheteau J, Bonin J (1973) Plate tectonics. Elsevier, Amsterdam 303 p

Mahmoud Y, Masson F, Meghraoui M, Cakir Z, Alchalbi A, Yavasoglu H, Yönlü O, Daoud M, Ergintav S, Inan S (2013) Kinematic study at the junction of the East Anatolian fault and the Dead Sea fault from GPS measurements. J Geodyn 67:30–39

Mann P, Hempton MR, Bradley DC, Burke K (1983) Development of pull-apart basins. J Geol 91:529–554
Marco S, Rockwell TK, Heimann A, Frieslander U, Agnon A (2005) Late Holocene activity of the Dead Sea Transform revealed in 3D paleoseismic trenches on the Jordan Gorge segment. Earth Planet Sci Lett 234:189–205
Marcus E, Slager J (1986) The sedimentary-magmatic sequences of Zemah-1 well (Dead Sea rift, Israel) and its emplacement in time and space. Isr J Earth Sci 34:1–10
Mart Y, Hall JK (1984) Structural trends in the northern Red Sea. J Geophys Res 89:11352–11364
Matmon A, Wdowinski S, Hall JK (2003) Morphological and structural relations in the Galilee extensional domain, northern Israel. Tectonophysics 371:223–241
McKenzie DP, Davies D, Molnar P (1970) Plate tectonics of the Red Sea and East Africa. Nature 224:125–133
Mechie J, Abu-Ayyash K, Ben-Avraham Z, El-Kelani R, Qabbani I, Weber M, DESIRE Group (2009) Crustal structure of the southern Dead Sea basin derived from DESIRE wide-angle seismic data. Geophys J Int 78:457–478. doi:10.1111/j.1365-246X.2009.04161.x
Meghraoui M, Gomez F, Sbeinati R, Van der Voerd J, Mouty M, Darkal A, Radan Y, Layyous I, Najjar HM, Darawcheh R, Hijazi F, Al-Ghazzi R, Barazangi M (2003) Evidence for 830 years of seismic quiescence from paleoseismology, archeoseismology and historical seismicity along the Dead Sea fault in Syria. Earth Planet Sci Lett 210:35–52
Meiler M, Reshef M, Shulman H (2011) Seismic depth-domain stratigraphic classification of the Golan Heights, central Dead Sea Fault. Tectopnophysics 510:354–369
Michelson H, Lipson-Benitah S (1986) The litho- and biostratigraphy of the southern Golan Heights. Isr J Earth Sci 35:221–240
Mittlefehldt D, Slager Y (1986) Petrology of the baslats and gabbros from the Zemah-1 drill hole, Jordan rift valley. Isr J Earth Sci 35:10–22
Mouty M, Delaloye M, Fontignie D, Piskin O, Wagner JJ (1992) The volcanic activity in Syria and Lebanon between Jurassic and Actual. Schwietz Mineralog Petrogt Mitt 72:91–105
Neev D, Hall JK (1979) Geophysical investigations in the Dead Sea. Sediment Geol 23:209–238
Nemer T, Meghraoui M (2006) Evidence for coseismic ruptures along the Roum Fault (Lebanon) a possible source of the AD 1837 earthquake. J Struct Geol 28:1483–1495
Nielsen C, Thybo H (2009) Lower crustal intrusions beneath the southern Baikal rift zone: evidence from full-waveform modelling of wide-angle seismic data. Tectonophysics 470:298–318
Over S, Ozden S, Unlugenc UC, Huseyin Yilmaz H (2004) A synthesis: late Cenozoic stress field distribution at northeastern corner of the Eastern Mediterranean, SE Turkey. Compt Rendus Geosci 336:93–103
Papazachos BC, Papaioannou CA (1999) Lithospheric boundaries and plate motions in the Cyprus area. Tectonophysics 308:193–204
Perinçek D, Çemen I (1990) The structural relationship between the East Anatolian and Dead Sea fault zones in southeastern Turkey. Tectonophysics 172:331–340
Petrunin A, Sobolev SV (2006) What controls thickness of sediments and lithospheric deformation at a pull-apart basin? Geology 34:389–392
Picard L (1943) Structure and evolution of Palestine, Bulletin of the Geology Department, Hebrew University. Geology Department, Hebrew University, Jerusalem, 187 p
Picard L, Baida U (1966) Geological report on the Lower Pleistocene deposits of the Ubeidiya excavations. Isr Acad Sci Hum Proc 4:1–16
Ponikarov VP (1964) Chief editor: the geologic map of Syria, Scale 1:1 000 000. Dept Geol Min Res Syria
Ponikarov VP, Kazmin VG, Kozlov VV, Krasheninnikov VA, Mikhailov IA, Razvlyaev AV, Soulidi-Kondratyev ED, Uflyand SK, Faradzhev VA (1969) Geology and mineral resources of foreign countries: Syria. Moscow, 216 p (in Russian)
Quennell AM (1959) Tectonics of the Dead Sea rift. 20th Int Geol Cong (1956), Assoc Afr Geol Surv pp 385–405
Reilinger R, McClusky S (2011) Nubia–Arabia–Eurasia plate motions and the dynamics of Mediterranean and Middle East tectonics. Geophys J Int 186:971–979

Reilinger R, 24 others (2006) GPS constraints on continental deformation in the Africa-Arabia-Eurasia continental collision zone and implications for the dynamics of plate interactions. J Geophys Res 111:B05411. doi:10.1029/2005JB004051

Renouard G (1955) Oil prospects of Lebanon. Am Assoc Petrol Geol Bull 39:2125–2169

Reznikov M, Ben-Avraham Z, Garfunkel Z, Gvirtzman H, Rotstein Y (2004) Structural and Stratigraphic framework of Lake Kinneret. Isr J Earth Sci 53:131–149

Robertson AHF (2001a) Mesozoic-Tertiary tectonic evolution of the Easternmost Mediterranean area: integration of marine and land evidence. Proc ODP Sci Results 160:723–782

Robertson AHF (2001b) Geological evolution of Cyprus, onshore and offshore evidence. In: Malpas J, Xenophontos C, Panayides A (eds) Proceedings of 3rd international conference on the geology of the eastern Mediterranean. Geological Survey Department, Nicosia, pp 11–44

Robertson AHF, Ünlügenç U, İnan N, Tasli K (2004) Missis-Andirin Complex: mélange formation related to closure and collision of the south-Tethys, in South Turkey. J Asian Earth Sci 22:413–453

Roeser HA (1975) A detailed magnetic survey of the southern Red Sea. Geol Jahrb D13:131–153

Rojay B, Heimann A, Toprak V (2001) Neotectonic and volcanic characteristics of the Karasu fault zone (Anatolia, turkey): the transition zone between the Dead Sea transform and the East Anatolian fault zone. Geodin Acta 14:197–212

Ron H (1987) Deformation along the Yammouneh, the restraining bend of the Dead Sea transform: paleomagnetic data and kinematic implications. Tectonics 9:1421–1432

Ron H, Freund R, Garfunkel Z, Nur A (1984) Block rotation by strike-slip faulting: structural and paleomagnetic evidence. J Geophys Res 89:6256–6270

Rotstein Y, Bartov Y (1989) Seismic reflection across a continental transform: an example from a convergent segment of the Dead Sea rift. J Geophys Res 94:2902–2912

Rotstein Y, Bartov Y, Frieslander U (1992) Evidence for local shifting of the main fault and changes in the structural setting, Kinnarot Basin, Dead Sea transform. Geology 20:251–254

Rukieh M, Trifonov VG, Dodonov AE, Minini H, Ammara O, Ivanova TP, Zaza T, Yusef A, Al-Shara M, Jobaili Y (2005) Neotectonic map of Syria and some aspects of Late Cenozoic evolution of the northwestern boundary zone of the Arabian plate. J Geodyn 40:235–256

Rybakov M, Fleischer L, Ten Brink U (2003) The Hula valley subsurface structure inferred from gravity data. Isr J Earth Sci 52:113–122

Ryberg T, Weber M, Garfunkel Z, Bartov Y (2007) The shallow velocity structure across the Dead Sea Transform fault, Arava Valley, from seismic data. J Geophys Res 112:B08307. doi:10.1029/2006JB004563

Sadeh M, Hamiel Y, Bock Y, Fang P, Wdowinski S (2012) Crustal deformation along the Dead Sea Transform and the Carmel Fault inferred from GPS measurements. J Geophys Res 117:B08410. doi:10.1029/2012JB009241

Saint-Marc P (1974) Etude stratigraphiqueet micropaleontologique de l'Albien, du Cenomanien et du Turonien du Liban. Notes et Memoirs de Moyen Orient 8:8–342

Şaroğlu F, Emre O, Kuşçu I (1992) The East Anatolian fault zone in Turkey. Ann Tecton Supplement to 6:99–125

Schattner U, Weinberger R (2008) A mid-Pleistocene deformation transition in the Hula basin, northern Israel: implications for the tectonic evolution of the Dead Sea Fault. Geochem Geophys Geosys 9, 18 p. doi:10.2029/2007GC001937

Schattner U, Ben-Avraham Z, Lazar M, Huebscher C (2006) Tectonic isolation of the Levant basin offshore Galilee-Lebanon – Effects of the Dead Sea fault plate boundary on the Levant continental margin, eastern Mediterranean. J Struct Geol 28:2049–2066

Schulman N (1962) The geology of the central Jordan Valley. Dissertation, Hebrew University, Jerusalem (in Hebrew)

Schütz F, Norden B, Forster A (2012) Thermal properties of sediments in southern Israel: a comprehensive data set for heat flow and geothermal energy studies heat flow. Basin Res 24:357–376

Searle MP (1994) Structure of the intraplate Eastern Plamyride fold belt, Syria. Geol Soc Am Bull 106:1332–1350

Segev A (1984) Lithostratigraphy and paleogeography of the marine Cambrian sequence in southern Israel and southwestern Jordan. Isr J Earth Sci 33:26–33
Segev A (2009) $^{40}Ar/^{39}Ar$ and K-Ar geochronology of Berriasian-Hauterivian and Cenomanian tectonomagmatic events in northern Israel: implications for regional stratigraphy. Cretac Res 30:810–828
Senel M (ed) (2002) The Geological map of Turkey, Sheet Hatay, 1:500 000. Direct Min Res Expl (MTA), Ankara
Şengör AMC, Yilmaz Y (1981) Tethyan evolution of Turkey: a plate tectonic approach. Tectonophysics 75:181–241
Şengör AMC, Gorur N, Saroglu F (1985) Strike-slip faulting and related basin formation in zones of tectonic escape; Turkey as a case study. Soc Econ Paleontol Mineral, Spec Publ 37:227–264
Şengör AMC, Görür N, Şaroĝlu F (2005) Strike slip faulting and related basin formation in zones of tectonic escape: Turkey as a case study. Soc Econ Plaeont Minerol Spec Publ 37:227–264
Seyrek A, Demir T, Pringle MS, Yurtmen S, Westaway RWC, Beck A, Rowbotham G (2007) Kinematics of the Amanos Fault, southern Turkey, from Ar/Ar dating of offset Pleistocene basalt flows: transpression between the African and Arabian plates. Geol Soc Lond Spec Publ 290:255–284. doi:10.1144/SP290
Shaliv G (1991) Stages in the tectonic and volcanic history of the Neogene basin in the Lower Galilee and the Valleys. Geol Surv Isr Report GSI/11/91, 100 p. (in Hebrew, Eng abs)
Sharkov EV (2000) Mesozoic and Cenozoic basaltic magmatism. In: Leonov, Yu G (eds) Outline of Geology of Syria. Rus Acad Sci, Geol Inst Trans, 526. pp 177–200. Nauka, Moscow (in Russian)
Shulman H, Reshef M, Ben-Avraham Z (2004) The structure of the Golan Heights and its tectonic linkage to the Dead Sea transform and the Palmyrides folding. Isr J Earth Sci 53:225–238
Smit J, Brun JP, Cloetingh S, Ben-Avraham Z (2010) The rift-like structure and asymmetry of the Dead Sea Fault. Earth Planet Sci Lett 290:74–82
Smit J, Brun JP, Cloetingh S, Ben-Avraham Z (2011) The rift-like structure and asymmetry of the Dead Sea Fault. Earth Planet Sci Lett 290:74–82
Sneh A, Weinberger R (2003) Geology of the Metulla quadrangle, northern Israel: implications for the offset along the Dead Sea rift. Isr J Earth Sci 52:123–138
Sobolev SV, Petrunin A, Garfunkel Z, Babeyko AY (2005) Thermo-mechanical model of the Dead Sea transform. Earth Planet Sci Lett 238:78–95
Steinitz G, Bartov Y (1991) The Miocene-Pliocene history of the Dead Sea segment of the rift in light of K-Ar ages of basalts. Isr J Earth Sci 40:199–208
Steinitz G, Bartov Y, Eyal M, Eyal Y (1981) K-Ar age determination of Tertiary magmatism along the western margin of the Gulf of Elat. Geol Surv Isr Curr Res 1980:27–29
Stern RJ (1994) Arc assembly and continental collision in the neoproterozoic E African Orogen: implications for the consolidation of Godwanaland. Ann Rev Earth Planet Sci 22:319–351
Suess E (1891) Die Brüche des östlichen Africa. Denkschrifte Akademie Wissenschaft Wien 58:555–584
Tatar O, Piper JDA, Gürsoy H, Heimann A, Koçulut F (2004) Neotectonic deformation in the transition zone between the Dead Sea Transform and the East Anatolian fault zone, southern Turkey: a palaeomagnetic study of the Karasu Rift volcanism. Tectonophysics 385:17–43
Ten Brink US, Ben-Avraham Z (1989) The anatomy of a pull-apart basin: seismic reflection observations of the Dead Sea basin. Tectonics 8:333–350
Ten Brink US, Flores CH (2012) Geometry and subsidence history of the Dead Sea basin: a case for fluid-induced mid-crustal shear zone? J Geophys Res 117:B01406. doi:10.1029/2011JB008711
Ten Brink US, Ben-Avraham Z, Bell RE, Hassouneh M, Coleman DF, Andersen G, Tibor G, Coakley B (1993) Structure of the Dead Sea pull-apart basin from gravity analysis. J Geophys Res 98:21877–21894
Ten Brink US, Rybakov M, Al Zoubi AS, Hassouneh M, Frieslander U, Batayneh AT, Goldschmidt V, Daoud MN, Rotstein Y, Hall JK (1999) Anatomy of the Dead Sea transform: does it reflect continuous changes in plate motion? Geology 27:887–890. doi:10.1130/0091-7613

Ten Brink US, Al Zoubi AS, Flores CH, Rotsterin Y, Qabbani I, Harder SH, Keller RG (2006) Seismic imaging of deep low velocity zone beneath the Dead Sea basin and transform faults: implications for strain localization and crustal rigidity. Geophys Res Lett 33:L24314. doi:10.1029/2006GL027890

Trifonov VG, Trubikhin VM, Adjamian J, Jallad Z, El-Khair Y, Ayad H (1991) The Levant fault zone in northwestern Syria. Geotectonics 2:63–75

Vidal N, Alvarez-Marron J, Klaeschen D (2000) Internal configuration of the Levantine Basin from seismic reflection data (Eastern Mediterranean). Earth Planet Sci Lett 180:77–89

Walley CD (1983) The paleoecology of the Callovian-Oxfordian strata of Majdal Shams (Syria) and its implications for Levantine palaeogeography and tectonics. Palaeogeogr Palaeoclim Palaeoecol 42:323–340

Walley CD (1988) A braided strike-slip model for the northern continuation of the Dead Sea fault and its implications for Levantine tectonics. Tectonophysics 1456:63–72

Walley CD (1998) Some outstanding issues in the geology of Lebanon and their importance in the tectonic evolution of the Levantine region. Tectonophysics 298:37–62

Weber M, DESERT Working Group (2004) The crustal structure of the Dead Sea transform. Geophys J Int 156:655–681. doi:10.1111/j.-1365/246X-2004.020143.x

Weber M, DESERT working Group (2009) Anatomy of the Dead Sea transform from lithospheric to microscopic scale. Rev Geophys 47:RG2002. doi:10.1029/2008RG000264

Weinberger R, Sneh A, Harlavan Y (2003) The occurrence of Middle-Miocene volcanism at Mount Hermon, northern Israel. Isr J Earth Sci 52:179–184

Weinberger R, Gross MR, Sneh A (2009) Evolving deformation along a transform plate boundary: example from the Dead Sea Fault in northern Israel. Tectonics 28:TC5005. doi:10.1029/2008TC002316

Weinberger R, Schattner U, Medvedev B, Frieslander U, Sneh A, Harlavan Y, Gross MR (2011) Convergent strike–slip across the Dead Sea Fault in northern Israel, imaged by high-resolution seismic reflection data. Isr J Earth Sci 58:203–216. doi:10.1560/IJES.58.3-4.203

Weinstein Y (2012) Transform faults as lithospheric boundaries, an example from the Dead Sea Transform. J Geodyn 54:21–28

Westaway R (2003) Kinematics of the Middle East and Eastern Mediterranean. Turk J Earth Sci 12:5–46

Westaway R, Arger J (1996) Gölbaşi basin, southeastern Turkey: a complex discontinuity in a major strike-slip fault zone. J Geol Soc Lond 153:729–744

Westaway R, Demir T, Seyrek A, Beck A (2006) Kinematics of active left-lateral faulting in SE Turkey from offset Pleistocene river gorges: improved constraint on the rate and history of relative motion between the Turkish and Arabian plates. J Geol Soc Lond 163:149–164. doi:10.1144/0016-764905-030

Wilson JT (1965) A new class of faults and their bearing on continental drift. Nature 207:343–347

Wu JE, Ken McClay K, Whitehouse A, Dooley T (2009) 4D analogue modelling of transtensional pull-apart basins. Mar Pet Geol 6:1608–1623

Yilmaz Y (1993) New evidence and model on the evolution of the southeast Anatolian orogen. Geol Soc Am Bull 105:251–271

Zak I (1967) The geology of Mount Sedom. Thesis Hebrew University of Jrusalem, 208p (in Hebrew, English abstract)

Zanchi A, Crosta GB, Darkal AN (2002) Paleostress analyses in NW Syria: constraints on the Cenozoic evolution of the northwestern margin of the Arabian plate. Tectonophysics 357:255–278